Energy Conversion and Management 262 (2022) 115649

Contents lists available at ScienceDirect

Energy Conversion and Management

journal homepage: www.elsevier.com/locate/enconman

Delivering net-zero carbon heat: Technoeconomic and whole-system comparisons of domestic electricity- and hydrogen-driven technologies in the UK

Andreas V. Olympios [a], Marko Aunedi [b], Matthias Mersch [a,c], Aniruddh Krishnaswamy [a], Corinne Stollery [a], Antonio M. Pantaleo [a,d], Paul Sapin [a], Goran Strbac [b], Christos N. Markides [a,*]

[a] Clean Energy Processes (CEP) Laboratory and Centre for Process Systems Engineering (CPSE), Department of Chemical Engineering, Imperial College London, London SW7 2AZ, UK
[b] Department of Electrical and Electronic Engineering, Imperial College London, London SW7 2AZ, UK
[c] Centre for Environmental Policy, Imperial College London, London SW7 2AZ, UK
[d] Department of Agro-environmental Sciences, University of Bari, 70121 Bari, Italy

ARTICLE INFO

Keywords:
Domestic heating
Electrification
Energy system
Heat pump
Hydrogen
Net zero

ABSTRACT

Proposed sustainable transition pathways for moving away from natural gas in domestic heating focus on two main energy vectors: electricity and hydrogen. Electrification would be implemented by using vapour-compression heat pumps, which are currently experiencing market growth in many countries. On the other hand, hydrogen could substitute natural gas in boilers or be used in thermally–driven absorption heat pumps. In this paper, a consistent thermodynamic and economic methodology is developed to assess the competitiveness of these options. The three technologies, along with the option of district heating, are for the first time compared for different weather/ambient conditions and fuel-price scenarios, first from a homeowner's and then from a whole-energy system perspective. For the former, two-dimensional decision maps are generated to identify the most cost-effective technologies for different combinations of fuel prices. It is shown that, in the UK, hydrogen technologies are economically favourable if hydrogen is supplied to domestic end-users at a price below half of the electricity price. Otherwise, electrification and the use of conventional electric heat pumps will be preferred. From a whole-energy system perspective, the total system cost per household (which accounts for upstream generation and storage, as well as technology investment, installation and maintenance) associated with electric heat pumps varies between 790 and 880 £/year for different scenarios, making it the least-cost decarbonisation pathway. If hydrogen is produced by electrolysis, the total system cost associated with hydrogen technologies is notably higher, varying between 1410 and 1880 £/year. However, this total system cost drops to 1150 £/year with hydrogen produced cost-effectively by methane reforming and carbon capture and storage, thus reducing the gap between electricity- and hydrogen-driven technologies.

1. Introduction

Major economies around the world have committed to net-zero carbon emissions by 2050 [1]. The building sector is responsible for more than one-third of global carbon emissions, half of which are attributed to space heating and hot-water provision [2]. For heating provision to be net-zero carbon, it should be either based solely on emission-free renewable energy technologies, or, in the case that some emissions occur, these should be fully offset [3]. Currently, domestic heating in many countries is dominated by fossil fuel technologies. For example, gas boilers are installed in more than 85% and 90% of homes in the UK [4] and the Netherlands [5], respectively. More than 60% of domestic heating in economies such as Germany, France, Belgium and Italy is also based on oil and gas systems [6]. The main technologies that are being proposed to replace gas boilers are electric heat pumps [7] and hydrogen boilers [8], which are locally carbon–neutral technologies.

Electric vapour-compression heat pumps are a mature technology that recently experienced significant market growth in many industrialised countries such as France and Germany, while the uptake in the UK remains low (0.25 million in total) [9]. These heat pumps use electricity to transfer heat from a cold source (e.g., ambient air or the ground) to a

* Corresponding author.
E-mail address: c.markides@imperial.ac.uk (C.N. Markides).

https://doi.org/10.1016/j.enconman.2022.115649

Available online 30 April 2022

Nomenclature

Abbreviations

AHP	absorption heat pump
ATR	autothermal reforming
BECCS	bioenergy with carbon capture and storage
BEIS	Department of Business, Energy & Industrial Strategy
CAPEX	capital expenses
CCC	Climate Change Committee
CCGT	combined cycle gas turbines
CCS	carbon capture and storage
CF	counterfactual
CHP	combined heat and power
COP	coefficient of performance
DH	district heating
DSM	demand-side management
EHP	electric heat pump
GUE	gas utilisation efficiency
HB	hydrogen boiler
IEA	International Energy Association
LCOH	levelised cost of heat
NECP	National Energy and Climate Plans
NET	negative emission technologies
OCGT	open cycle gas turbines
OPEX	operating expenses
PEM	proton exchange membrane
PHE	plate heat exchanger
PVGIS	Photovoltaic Geographical Information System
SHX	solution heat exchanger
SMR	steam methane reforming
WeSIM	Whole-electricity System Investment Model

Greek symbols

α	local heat transfer coefficient (W/m^2/K)
β	chevron angle (rad)
Δ	difference (-)
δ	thickness (m)
ε	heat exchanger effectiveness (-)
η	efficiency (-)
Λ	wavelength of corrugation (m)
λ	excess air ratio (-)
μ	dynamic viscosity (Pa.s)
ρ	density (kg/m^3)
σ	surface tension (N/m)

Symbols

A	area (m^2)
Bo	boiling number (-)
C	cost (£)
c	concentration (kg/m^3)
c_p	specific heat capacity (J/kg/K)
d	diameter (m)
f	solution circulation ratio (-)
G	mass velocity (kg/m^2/s)
H	height (m)
h	specific enthalpy (J/kg)
HV	lower heating value (J/kg)
i	inflation rate (-)
L	latent heat of vaporisation (J/kg)
l	length (m)
M	molar mass (kg/mol)
$\dot{m}$	mass flowrate (kg/s)
n	technology lifetime (years)
$\dot{n}$	molar flowrate (mol/s)
Nu	Nusselt number (-)
P	pressure (Pa)
Pr	Prandtl number (-)
r	discount rate (-)
$\dot{Q}$	heat transfer rate (W)
q	vapour quality (-)
Re	Reynolds number (-)
S	spacing (m)
T	temperature (K)
U	overall heat transfer coefficient (W/m^2/K)
$\dot{V}$	volumetric flowrate (m^3/s)
$\dot{W}$	work output (W)
w	width (m)
x	mass fraction (-)

Subscripts

abs	absorber
ahp	absorption heat pump
ann	annual
boil	boiler
c	cold
Car	Carnot
chan	channel
comp	compressor
cond	condenser
dem	demand
ehp	electric heat pump
eq	equivalent
evap	evaporator
exe	exergetic
ext	external
fc	forced convection
fg	flue gas
fr	frontal
gen	generator
H	hydraulic
h	hot
in	inlet
int	internal
is	isentropic
i	fluid stream
j	heat exchanger section
L	latent heat
l	liquid
lg	log-mean
loss	losses from boiler
nb	nucleate boiling
o	overall
out	outlet
pp	pinch-point
pump	electric pump
S	sensible heat
sat	saturation
sh	superheating
shx	solution heat exchanger
sol	solution
tot	total
w	wall
wf	working fluid
v	vapour

hot sink (e.g., internal space of buildings or hot water), and are associated with considerably better thermodynamic performance and longer lifespan than widely used gas boilers [10]. Their performance is evaluated using the coefficient of performance (COP), defined as the heat delivered per unit electricity consumed. In the case of hot-water provision, the COP of an air-source heat pump varies between ~ 1.5–4 for outside air temperatures between −15 °C and 20 °C [11].

In the 'Net Zero' advice report published by the UK Climate Change Committee (CCC) [3] to provide recommendations to the government, electrification is suggested as the key route to achieve decarbonisation targets. Achieving this is challenging for two reasons: (i) in order to provide net-zero carbon heat through electric heat pumps, the electricity required must itself be net-zero carbon; and (ii) electrifying the whole building sector will have significant implications on the total electricity demand, which could increase by 50% to 2050 [3]. If accompanied with electrified transport, the total electricity demand is expected to roughly double by 2050, reaching close to 600 TWh/year [3].

Wilson et al. [12] demonstrated that a large uptake of heat pumps would lead to remarkable upgrade requirements for the existing network infrastructure mainly because of a considerable rise in peak electricity requirements. It is therefore vital that electrification is accompanied with measures that can reduce the overall heat-driven electricity demand and can provide flexibility by reducing daily peak demands. Such measures involve improvements in building energy efficiency [13] and demand-side management (DSM), either through behavioural changes [14] or energy storage (at a household level in small batteries [15] and thermal stores [16] or at a grid level in long-duration, large-scale systems [17]).

Hydrogen is proposed as the major alternative to electrification for the delivery of low-carbon heating to buildings. It benefits from the potential of repurposing the existing natural gas distribution infrastructure to supply hydrogen. However, this transformation would involve additional costs related to new transmission pipelines, additional compressors and replacement of certain distribution pipelines [18]. Converting the gas network to 100% hydrogen would happen gradually, with current plans in the UK [19] and Germany [20] involving an initial blending of hydrogen into the existing gas network at small proportions (20%) to demonstrate safety and to close any knowledge gaps.

Hydrogen boilers, like natural gas boilers, involve the combustion of a gas to produce heat. Therefore, these two technologies share similar efficiencies and many identical components. A few differences involve the design of the burner and the flame detector, which should be specifically designed for each fuel. The cost differences between these components are expected to be small, with major boiler manufacturers suggesting recently (perhaps arguably) that, at current volumes, hydrogen boilers will cost no more than natural gas equivalents for domestic consumers [21].

In a net-zero context, hydrogen can be produced by water electrolysis, or by methane reforming with carbon capture and storage (CCS) [22]. In the case that it is produced by steam methane reforming (SMR) or auto-thermal reforming (ATR), the CO_2 emissions associated with these technologies should be minimised, and any residual emissions should be offset using negative-emission technologies (NETs) [23]. Although SMR has been commercially used for many years, the potential broad use of hydrogen in net-zero energy systems has led to several new studies and advancements in the design of emerging reforming technologies. Various authors have examined the role of different conditions (e.g., CO_2 concentration) on performance and, specifically, CO_2 capture rates. Furthermore, instead of using backend CO_2 capture processes [24], emerging options involve sorption-enhanced SMR systems, which combine hydrogen production and in-situ CO_2 capture [25]. The latter technology involves various design [26] and operation options [27].

Developing a "thriving" low-carbon hydrogen sector is a key component of the UK government's plans. A recent strategy report [28] mentions the start of a trial neighbourhood heated by hydrogen by 2023, followed by a village trial by 2025 and potentially a town pilot project by 2030. Sunny et al. [8] conducted an assessment of regional transitions from existing natural gas supply chains to hydrogen-based infrastructure. The authors concluded that the most cost-effective hydrogen-based heat supply would involve deploying ATR with CCS and NETs, using salt caverns to store hydrogen and other geological reservoirs for CO_2 storage. In addition, Northern Gas Networks commissioned a feasibility study – the "H21 project" [29] – to examine the feasibility of converting the gas grid in the north of England to 100% hydrogen and outlined the need for detailed engineering design of hydrogen technologies.

Absorption heat pumps, like their electric counterparts, extract renewable heat from a low-temperature heat source (e.g., ambient air), but instead of using an electrically-powered compressor, they are thermally driven. Absorption systems have been widely studied for refrigeration purposes and are gaining increased attention for heating applications. Scoccia et al. [30] used experimental data collected from a prototype designed for residential applications [31] to show that, in countries where electricity prices are much higher than gas prices, gas-driven absorption heat pumps can potentially lead to higher savings than electric heat pumps. Furthermore, Lu et al. [32] conducted a thermoeconomic analysis of a gas-fired absorption heat pump aimed at a high-temperature hot-water application and concluded that the average payback period in south China is as low as 3 years.

An absorption heat pump system requires two fluids: an absorber and a refrigerant. Water (H_2O) and lithium bromide (LiBr) are one of the most common pairs, but their use in low-temperature applications is limited due to solution crystallisation and a high refrigerant freezing point, which makes them unsuitable for heat-source temperatures below 5 °C at the evaporator [33]. This is impractical in most space heating and hot-water provision applications. Another suitable pair option involves ammonia (NH_3) and water (H_2O). This is associated with low leakage, no crystallisation, and the ability to use sub-zero evaporator temperatures [34,35], and is thus widely used in refrigeration [36] and heating applications [37].

Similar to electric heat pumps, the performance of absorption heat pumps is measured by the COP, but in this case the indicator is defined as the ratio of the useful heat output to the required (combined) heat and electrical inputs, where the latter is required to operate a circulation pump. Since heat input is provided by a fuel (e.g., gas) in most cases, another common measure of performance is the gas utilisation efficiency (GUE) [38], also sometimes referred to as heat-to-fuel ratio [39], which is equal to the COP multiplied by the combustion efficiency (85–94% for modern gas-fired boilers [40]). Scoccia et al. [30] demonstrated that the GUE of residential gas-fired ammonia-water absorption heat pumps can vary between 0.9 and 1.7 for air temperatures between –20 °C and 25 °C and hot-water temperatures from 25 °C to 60 °C. Garrabrant et al. [41] measured a COP in the range 1.44–1.63 when supplying hot water at 45 °C at an ambient temperature of 20 °C. In addition, Wu et al. [33] developed a prototype that can operate successfully under evaporator inlet temperatures as low as –18 °C (when the heat source is calcium chloride). In that work, the authors predicted a COP between 1.43 and 1.55 when supplying hot water at 45 °C with a heat-source water inlet temperature of 15 °C.

The literature to-date lacks an assessment of the potential of hydrogen-driven absorption heat pumps in a wider hydrogen-based economy. This technological solution would be based on mature components (i.e., heat exchangers, valves, pumps); the only difference compared to existing gas-fired absorption technologies would be that the required heat should be provided by a hydrogen boiler rather than a natural gas boiler. In the summary report of the International Energy Association (IEA) Heat Pump Technology Collaboration Programme on thermally-driven heat pumps [42], it is stated that "gas heat pumps would be compatible with hydrogen in any repurposed gas grid", and that this could be a factor to make the case for government intervention and further technology development and deployment.

Table 1
Advantages and disadvantages of the main technology candidates for domestic heating decarbonisation.

Technology	Advantages	Disadvantages
Electric heat pumps	• Mature technology • Better performance than boilers • Long lifespan	• Higher price than boilers • Electricity must itself be net-zero carbon • Significant grid upgrade requirements
Hydrogen boilers	• Proven technology for all building types • Many identical components to gas boilers • Potential of repurposing the gas grid	• Higher operational costs than heat pumps • Technologies for net-zero carbon hydrogen production are not yet mature • Expensive infrastructure transformation
Hydrogen-driven absorption heat pumps	• Based on mature components • Same fuel as boilers but higher efficiency • Gas-driven heat pumps are compatible	• Higher price than boilers • Technologies for net-zero carbon hydrogen production are not yet mature • Expensive infrastructure transformation

A summary of the main advantages and disadvantages associated with the discussed technology candidates for the decarbonisation of domestic heating is presented in Table 1.

A comprehensive technoeconomic comparison of domestic electricity and hydrogen-driven heating technologies that captures how their performance and cost depend on their components and operating conditions, has not been presented in literature so far. Thus, the first novelty of this work is in the development of thermodynamic and component-costing models of a vapour-compression heat pump, a standalone hydrogen boiler and an absorption heat pump driven by heat from a hydrogen boiler. In particular, and to the best of the authors' knowledge, the potential of the latter technology has never been explored using comprehensive design and costing methods in the context of heating decarbonisation through hydrogen. For technologies involving similar components (electric and absorption heat pumps), consistent modelling assumptions and cost correlations are used, providing a like-to-like comparison.

When comparing candidate heating technologies from a homeowner's perspective, results for different locations vary due to weather conditions, but also, importantly, due to the difference in the relative prices of fuels and electricity. A gap has been identified in the literature in assessing the competitiveness of different options for varying relative fuel prices. Therefore, the second novelty of this work lies in the technoeconomic comparison of the main low-carbon heating technology candidates for a range of electricity and hydrogen prices. A direct comparison to district heating (DH) is also provided for a range of DH prices, as this is another available option for certain households.

The analysis focuses on the UK as a case study. The UK is one of the countries with the lowest uptake of heat pumps and the highest electricity-to-gas price ratios in Europe [9], making it an example of a country where government intervention is vital to ramp up the installation of low-carbon heating technologies. Furthermore, since the comparison is conducted for various prices of hydrogen and electricity, insights can also be obtained for countries with different energy-price characteristics.

Comparing domestic heating technologies from the homeowner's perspective can be useful to assess how the government can develop policy programmes to support the uptake of technologies that best align with the country's environmental and economic objectives. To quantify the latter, however, it is necessary to investigate how different heating technologies compare in the context of a whole-energy system perspective. Therefore, the third novelty of this work is the integration of the developed technology models within the Whole-electricity System Investment Model (WeSIM), a model of the whole UK energy system [43], which has recently been used to provide, along with the CCC, evidence to the government on heating decarbonisation [44]. WeSIM is here used to identify the minimum decarbonisation transition cost and future technology mix in the UK that are associated with each of the modelled heating options.

Section 2 includes a description of the thermodynamic and component-costing models of the heating technologies under investigation, as well as of the utilised whole-energy system model. In Section 3, the results of the technoeconomic comparison from the homeowner's and energy-system perspectives are presented and discussed. Lastly, concluding remarks are provided in Section 4.

2. Methods

The domestic heating decarbonisation pathways considered in this paper include three technology options, as shown in Fig. 1: (i) a vapour-compression heat pump driven by electricity; (ii) a standalone hydrogen boiler; and (iii) an ammonia-water absorption heat pump driven by heat from a hydrogen boiler. The performance of these technologies varies with operating conditions; therefore, a wide uptake of each of them would have different effects on the country's technology mix. In this section, the thermodynamic and component-costing technology models, as well as the whole-energy system model used to assess the system implications associated with a wide uptake of these technologies, are presented in detail.

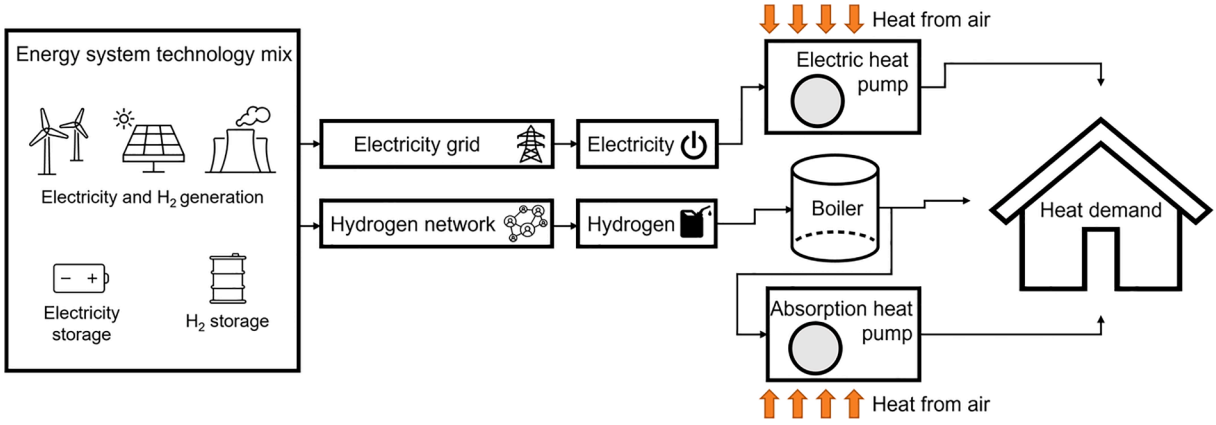

Fig. 1. Schematic diagram of investigated electricity- and hydrogen-driven domestic heating options. A wide uptake of each of these options would require drastic and different changes to the country's energy system technology mix.

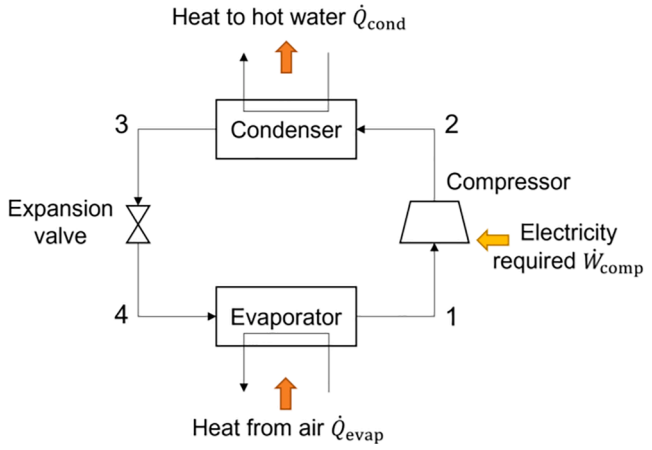

Fig. 2. Basic architecture of an electric heat pump. Electrical power is provided in the compressor to compress vapour and transfer heat from a cold region (i.e., outside air) to a hot region (hot water).

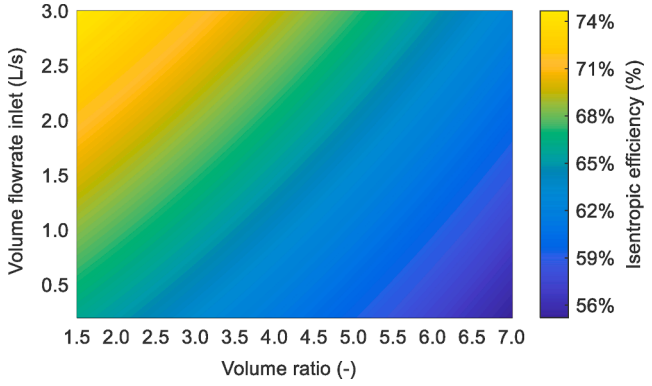

Fig. 3. Rotary-vane compressor performance map (isentropic efficiency as a function of volume flowrate at the inlet and volume ratio). The map represents the best fit between the off-design performance curves of 30 hermetic rotary vane compressors found on the UK market in 2021.

2.1. Electric heat pump model

The basic architecture of an electric heat pump is shown in Fig. 2. In its simplest form, this comprises four main components: a condenser, an expansion valve, an evaporator and a compressor. Heat is transferred from the heat source to a working fluid in the evaporator. The low-pressure vapour refrigerant leaving the latter is compressed by a compressor, delivering high-temperature high-pressure vapour, which is then cooled and condensed in the condenser. The high-pressure low-temperature liquid at the condenser outlet undergoes a Joule-Thomson expansion in the expansion valve before being sent to the evaporator as a low-temperature low-pressure liquid. The heat rejected in the condenser is recovered by a hot-water circuit and used to provide space heating and/or to fulfil a household's hot water demand.

A validated spatially-lumped model of an electric heat pump based on a single-stage compressor was developed in previous work by the authors [11,45]. The model, which assumes steady-state operation of components, isenthalpic expansion through the expansion valve and negligible pressure and heat losses in heat-exchange components and pipes, was validated based on an analysis of more than 100 electricity-driven air-source heat pumps available on the UK market. R410a was identified as the most used working fluid in recent years (in more than 70% of the cases) [46], but there is a clear trend towards a switch to R32, which exhibits better performance [47,48] and much lower global warming potential (675 compared to 2088 for R410a [49]). The market analysis also shows that most small-scale (<10 kW_{th}) electric heat pumps use hermetic rotary vane compressors, while scroll compressors are seldom used.

Based on the market analysis, in this work the working fluid is chosen to be R32. Furthermore, the electric heat pump model described in detail in the authors' previous studies is extended to include a new compressor efficiency map using data collected from 30 hermetic rotary vane compressors found on the UK market in 2021 [50]. The performance map, which is plotted in Fig. 3, shows the isentropic efficiency as a function of the compressor's volume ratio and inlet volumetric flowrate. The map represents the best fit between the off-design performance of the compressors under investigation, meaning that it represents the off-design performance of an average small-scale rotary vane compressor.

The working fluid enters the compressor (Process 1–2 in Fig. 2) at a specific enthalpy h_1, and is compressed up to a high pressure, P_2. For an isentropic efficiency $\eta_{is,\,comp}$, calculated from the rotary-vane-compressor performance map, the enthalpy at the outlet of a well-insulated compressor h_2 is:

$$h_2 = h_1 + \frac{h_{2,is} - h_1}{\eta_{is,\,comp}}, \tag{1}$$

where $h_{2,is}$ is the specific outlet enthalpy for an isentropic compression process. The electricity required to operate the compressor, $\dot{W}_{comp}$, is calculated as:

$$\dot{W}_{comp} = \dot{m}_{wf}(h_2 - h_1) = \frac{\dot{m}_{wf}(h_{2,is} - h_1)}{\eta_{is,comp}}, \tag{2}$$

where $\dot{m}_{wf}$ is the mass flowrate of the working fluid.

Energy balance equations are written for each component [51] to obtain the heat transfer rate by the heat source to the working fluid in the evaporator and by the working fluid to the heat sink in the condenser.

In this work, the degree of superheating at the evaporator outlet (controlled by the expansion valve setting) is assumed constant and equal to 5 K and the condenser outlet liquid is assumed saturated (i.e., no subcooling). A 5-K pinch-point temperature difference is assumed in all heat exchangers for design purposes. A detailed analysis of the model formulation can be found in Refs. [11,45]. The COP of the electric heat pump, COP_{ehp}, is the ratio of the heat output, $\dot{Q}_{cond}$, to the electricity input, $\dot{W}_{comp}$ [11]:

$$COP_{ehp} = \frac{\dot{Q}_{cond}}{\dot{W}_{comp}}. \tag{3}$$

Furthermore, the exergetic efficiency of the heat pump, which is the ratio of the total exergy output to the total exergy input, is also equal to the heat pump's COP over the theoretically maximum Carnot COP, and is calculated here following Refs. [52,53] from:

$$\eta_{ehp,exe} = \frac{COP_{ehp}}{COP_{ehp,Car}} = \frac{\dot{Q}_{cond}}{\dot{W}_{comp}}\left(1 - \frac{T_{air}}{T_{dem}}\right), \tag{4}$$

where T_{dem} is the hot-water demand temperature and T_{air} the temperature of the outside air.

2.2. Hydrogen boiler model

In this work, a catalytic hydrogen boiler is selected for investigation. Catalytic boilers are flameless heaters that convert fuel and air into reaction products through catalysed chemical reactions, resulting in negligible emissions [54]. A hydrogen boiler can be modelled as a reaction chamber and a separate heat exchanger that heats water. The model here is based upon a modified natural gas boiler [55], assuming that the reaction of hydrogen with dry air is complete and that all components operate at steady-state conditions.

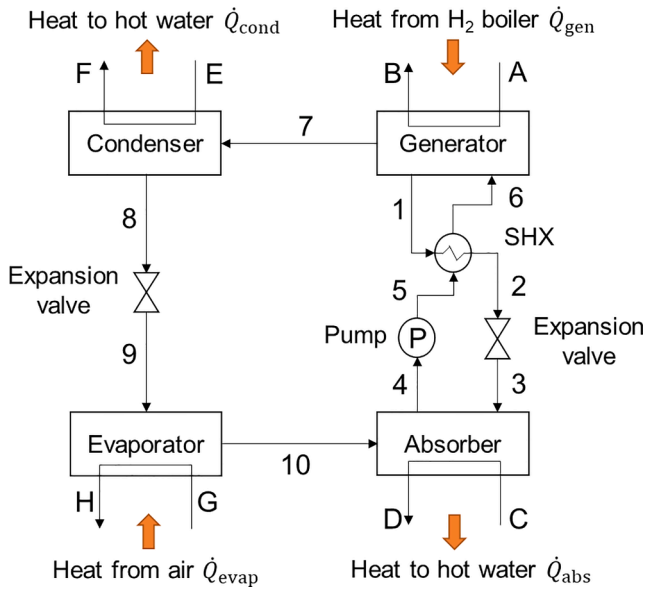

Fig. 4. Basic architecture of an absorption heat pump. Vapourised refrigerant out of the evaporator is absorbed by the absorber, forming a liquid solution, which is pumped to the generator. Heat from a hydrogen boiler is supplied in the generator to retrieve the refrigerant from the liquid solution.

The reaction taking place in the reaction chamber is as follows [56]:

$$H_2 + \frac{\lambda}{2}(O_2 + 3.76N_2) \rightarrow H_2O + \frac{(\lambda - 1)}{2}O_2 + \frac{3.76\lambda}{2}N_2, \tag{5}$$

where λ is the excess air ratio (=1.13, in line with observed values in boilers [55]) and 3.76 represents the ratio of nitrogen to oxygen in air. Consequently, the total molar flowrate of the flue gases out of the chamber is the sum of the coefficients of the products, multiplied by the molar flowrate of hydrogen:

$$\dot{n}_{fg} = \dot{n}_{H_2}\left(1 + \frac{\lambda - 1}{2} + \frac{3.76\lambda}{2}\right). \tag{6}$$

The mole fraction of each product in the flue gases is equal to that product's molar flowrate divided by the total flowrate of the flue gases. Hydrogen reacts in the catalytic boiler at around 300 °C [57]. A weighted flue gas molar heat capacity $\overline{C_{p_{fg}}}$ is estimated by summing the multiples of the mole fractions of each product and their respective molar heat capacity. Energy is lost from the combustion process in the flue gas as sensible heat (Equation (7)) and latent heat in water vapour (Equation (8)):

$$\dot{Q}_{fg,S} = \dot{n}_{fg}\overline{c_{p_{fg}}}(T_{fg} - T_0); \tag{7}$$

$$\dot{Q}_{fg,L} = \dot{n}_{fg}x_{H_2O}M_{H_2O}L_{H_2O}, \tag{8}$$

where x_{H_2O} is the mole fraction of water in the flue gas stream, M_{H_2O} the molar mass of water, L_{H_2O} the latent heat of vaporisation of water, T_{fg} the temperature of the flue gases and T_0 the temperature of the environment. Summing these two effects gives:

$$\dot{Q}_{fg} = \dot{Q}_{fg,S} + \dot{Q}_{fg,L}. \tag{9}$$

The amount of fuel energy required to run the boiler is calculated using:

$$\dot{Q}_{fuel} = \dot{Q}_{out} + \dot{Q}_{fg} + \dot{Q}_{loss}, \tag{10}$$

where $\dot{Q}_{out}$ is the heat supplied from the boiler and $\dot{Q}_{loss}$ accounts for heat losses from the boiler structure (approximated to be 1% of the sum of $\dot{Q}_{out}$ and $\dot{Q}_{fg}$). In condensing boilers, the water vapour in the products is condensed and therefore the losses are reduced. $\dot{Q}_{fuel}$ can be divided by the lower heating value of hydrogen, HV_{fuel}, to provide the required mass flowrate of hydrogen into the boiler:

$$\dot{m}_{fuel} = \frac{\dot{Q}_{fuel}}{HV_{fuel}}. \tag{11}$$

2.3. Hydrogen-driven absorption heat pump model

The compressor used in a mechanical vapour-compression heat pump is replaced with an absorption cycle in an absorption heat pump. The absorption cycle consists of a generator, a solution heat exchanger (SHX), an absorber, an electricity-driven pump and an expansion valve. A schematic diagram of the ammonia-water absorption heat pump is shown in Fig. 4. The high-pressure components are the condenser, generator and SHX, and the low-pressure components are the evaporator and absorber. The principle of operation is that the vapourised refrigerant (in this case ammonia) leaving the evaporator is absorbed by the absorbent (in this case water), forming a liquid solution that is then pumped to the high-pressure components. The pumping process requires a negligible amount of electricity compared to that required to compress vapour in electric heat pumps. Heat from the high-temperature source (in this case a hydrogen boiler) is supplied to the system in the generator to desorb the refrigerant from the liquid solution. The SHX is used to improve the system's performance by preheating the solution.

Referring to Fig. 4, Stream 1 represents the 'weak' ammonia-water solution, a high-pressure subcooled liquid with low ammonia content following the heat input from the hydrogen boiler in the generator. Stream 1 enters the counter-flow SHX and following this, Stream 2 enters the expansion valve and exits as a low-pressure saturated liquid, Stream 3. Stream 4 is the 'strong' refrigerant solution, a saturated liquid containing a large amount of ammonia, pumped to high pressure using the pump (P). Stream 5 is preheated in the SHX by recovering heat from the weak solution and exits as Stream 6 to feed the generator. High-pressure saturated refrigerant vapour exits the generator in Stream 7 and condenses into a high-pressure liquid in Stream 8, which then flows through another expansion valve to reduce its pressure. The resulting low-pressure liquid (Stream 9) then recovers heat from ambient air and leaves the evaporator as a low-pressure vapour (Stream 10), which finally feeds the absorber. Streams A and B represent the hot-water loop to the hydrogen boiler, while Streams C, D, E and F are the water-supply streams for household heating. Stream C is heated by heat being released by the absorption process and Stream E is heated by the condensation of the refrigerant in the condenser. Streams G and H represent the ambient air, from which low-grade heat is drawn.

The thermodynamic model is developed in MATLAB [58] and thermophysical equilibrium and transport properties are extracted from REFPROP [59]. For ammonia-water mixtures with more than 5% of water, the models developed by Conde-Petit [60] are used. Like for the electric heat pump, the model assumes that flow-throttling processes through valves are isenthalpic (though incur a temperature change due to the Joule-Thomson effect), all components operate at steady-state conditions and there are negligible pressure and heat losses in components. The degrees of superheating and subcooling and the pinch-point temperature differences between the working fluid and heat sources/sinks are the same as for the electric heat pump model. In addition, the model assumes that the ammonia-water solution is saturated at the generator and absorber outlet, and ammonia leaving the condenser and evaporator is also saturated, which are widely used assumptions in absorption refrigeration models [61–64]. The SHX effectiveness factor is equal to 0.8 (same as in Ref. [63] and within the ranges considered in Refs. [64–67]). The generator-inlet temperature is set at 165 °C, which safely allows to operate with up to 90% ammonia-rich mixtures while maintaining a 10-K margin from the critical temperature. Lastly, the pump isentropic efficiency is 80% (this has minimum effect due to negligible power required).

The model is represented by Equations (12) to (30). Hereby, the indices of temperatures (T), pressures (P) and enthalpies (h) refer to the fluid streams as shown in Fig. 4. Detailed explanation of symbols is provided in the nomenclature. The temperatures of the outlet stream of the condenser, T_8, and absorber, T_4, are calculated using Equation (12). Assuming saturated liquid leaves the condenser, the pressure at its outlet is determined. This is equal to the pressure of all high-pressure components of the cycle:

$$T_8 = T_4 = T_d + T_{pp}; \tag{12}$$

$$P_{high} = P_{sat}(T_8) = P_8 = P_1 = P_2 = P_5 = P_6 = P_7. \tag{13}$$

The temperature of the evaporator-outlet stream is calculated using Equation (14), and assuming some degree of superheating, T_{sh}, the pressure of low-pressure components is determined:

$$T_{10} = T_{air} - T_{pp}\,; \tag{14}$$

$$P_{low} = P_{sat}(T_{10} - T_{sh})\, P_{10} = P_9 = P_3 = P_4. \tag{15}$$

The temperature of the weak solution is determined using Equation (16), where T_{gen} is the heat-source temperature. The concentrations of the strong and weak solutions required to obtain these temperatures and pressures are obtained and the enthalpy at the pump outlet is based on the isentropic efficiency:

$$T_1 = T_{gen} - T_{pp}; \tag{16}$$

$$h_5 = h_4 + \frac{(h_{5,ideal} - h_4)}{\eta}. \tag{17}$$

The SHX effectiveness, ε_{shx}, is used to calculate the temperature of Stream 2:

$$T_2 = T_1 - \varepsilon_{shx}(T_1 - T_5)\,. \tag{18}$$

Assuming isenthalpic expansion across the expansion valve, the enthalpy of Stream 3 is found:

$$h_3 = h_2\,. \tag{19}$$

The mass conservation equation satisfied in each component is expressed as:

$$\sum_i \dot{m}_{i,in} x_{i,in} - \sum_i \dot{m}_{i,out} x_{i,\,out} = 0\,. \tag{20}$$

where $\dot{m}$ represents mass flow rate and x the mass fraction. The solution circulation ratio f is defined as the ratio between the mass flowrate of the weak solution entering the generator and that of the refrigerant vapour leaving the generator [68]. Using Equation (20), the solution circulation ratio can be written as:

$$f = \frac{\dot{m}_6}{\dot{m}_7} = \frac{x_1}{x_1 - x_4}. \tag{21}$$

The energy balances for each component of the cycle are the following:

$$\dot{Q}_{gen} = \dot{m}_7 h_7 + \dot{m}_1 h_1 - \dot{m}_6 h_6; \tag{22}$$

$$\dot{Q}_{cond} = \dot{m}_7 (h_7 - h_8); \tag{23}$$

$$\dot{Q}_{evap} = \dot{m}_9 (h_{10} - h_9); \tag{24}$$

$$\dot{Q}_{abs} = \dot{m}_{10} h_{10} + \dot{m}_3 h_3 - \dot{m}_4 h_4; \tag{25}$$

$$\dot{Q}_{shx} = \dot{m}_5 (h_6 - h_5); \tag{26}$$

$$\dot{W}_{pump} = \dot{m}_4 (h_5 - h_4). \tag{27}$$

The flowrates of each stream of the cycle can be calculated by solving mass-conservation and energy-balance equations. The solution enthalpy at the generator inlet is thus obtained from:

$$h_6 = h_5 + \frac{\dot{m}_1}{\dot{m}_4}(h_1 - h_2). \tag{28}$$

In this idealised model, it is assumed that the temperature of the water outlet stream from the absorber is the same as that of the condenser, and that both are equal to the demand temperature. The heat output from both components is, thus, the useful heat for the supply water, and the COP of the absorption heat pump is thus given by:

$$COP_{ahp} = \frac{\dot{Q}_{abs} + \dot{Q}_{cond}}{\dot{W}_{pump} + \dot{Q}_{gen}}. \tag{29}$$

Lastly, based on exergy analysis (as per Refs. [69,70]), the exergetic efficiency of the heat pump is:

$$\eta_{ahp,exe} = \frac{\dot{Q}_{abs}\left(1 - \frac{T_{air}}{T_{dem}}\right) + \dot{Q}_{cond}\left(1 - \frac{T_{air}}{T_{dem}}\right)}{\dot{W}_{pump} + \dot{Q}_{gen}\left(1 - \frac{T_{air}}{T_{gen}}\right)}. \tag{30}$$

where $\dot{W}_{pump}$ is small and often neglected. Equations (29) and (30) represent the COP and exergetic efficiency of the absorption heat pump itself (i.e., they do not account for the energy/heat loss and exergy destruction in the hydrogen boiler that supplies heat to it).

Ammonia is highly toxic [71] and any parts of the system in contact with ammonia must be sufficiently proofed to limit breakage risk. In addition, especially when impurities are present, ammonia is corrosive, which means that rigid safety procedures should be ensured, and appropriate training must be undertaken by contractors to mitigate risks during installation and charging.

2.4. Electric and absorption heat pump heat exchanger sizing

Predicting the cost of domestic heating technologies requires the sizing of their components. The cost of heat exchangers can be represented as a function of the heat transfer area [72]. In domestic applications, where compactness is key, plate heat exchangers (PHEs), which are generally characterised by high performance and compactness, are nowadays the most commonly used type of heat exchanger in commercially available domestic heat pumps [11] and other small-scale applications [73]. In this work, all heat exchangers are assumed to be PHEs, except the evaporators, where plate fin-and-tube heat exchangers are used to increase the heat transfer area and enhance air-to-fluid heat transfer coefficients.

Heat exchangers are split into sections according to the occurring fluid phases (liquid, two-phase or vapour). The heat transfer area of each section (denoted with subscript 'j') is obtained from:

$$A_j = \frac{\dot{Q}_j}{U_j \Delta T_{lm,j}}, \tag{31}$$

where A is the heat transfer area, $\dot{Q}$ the heat flow, U the overall heat transfer coefficient and ΔT_{lm} the logarithmic mean temperature difference:

$$\frac{1}{U_j} = \frac{1}{\alpha_{h,j}} + \frac{\delta_w}{k_w} + \frac{1}{\alpha_{c,j}}; \tag{32}$$

$$\Delta T_{lm,j} = \frac{(T_{h,i} - T_{c,i}) - (T_{h,o} - T_{c,o})}{\ln \frac{T_{h,i} - T_{c,i}}{T_{h,o} - T_{c,o}}}, \tag{33}$$

where α is the local heat transfer coefficient, k_w the wall thermal conductivity and δ_w the wall thickness. Subscripts 'h' and 'c' represent the hot and cold streams, and subscripts 'i' and 'o' the inlet and outlet streams. The local heat-transfer coefficients α in each heat exchanger section j are determined from:

Table 2
Cost correlations for different components of the considered heating technologies and related variables.

Component	Dependent variable	Cost (£)	Ref.
Absorber	Heat exchange area A_{abs} (m^2)	$288 + 316\ A_{abs}$	[50]
Condenser	Heat exchange area A_{cond} (m^2)	$288 + 316\ A_{cond}$	[50]
Generator	Heat exchange area A_{gen} (m^2)	$288 + 316\ A_{gen}$	[50]
Solution heat exchanger	Heat exchange area A_{shx} (m^2)	$288 + 316\ A_{shx}$	[50]
Evaporator	Heat exchange area A_{evap} (m^2)	$288 + 217\ A_{evap}$	–
Compressor	Inlet volumetric flowrate $\dot{V}_{comp,in}$ (m^3/s)	$8370\ \dot{V}_{comp,in}^{0.456}$	[50]
Air fan	Frontal area A_{fr} (m^2)	$578\ A_{fr}$	[75]
Pump	Work required $\dot{W}_{pump}$ (kW)	$512\ \dot{W}_{pump}^{0.460}$	[11]
Valve	–	135	[77]
Miscellaneous hardware	Total cost of components C_{tot} (£)	$0.2\ C_{tot}$	[78]
Profit margin	Total cost of components C_{tot} (£)	$0.2\ C_{tot}$	[78]
Tax	Total cost of components C_{tot} (£)	$0.2\ C_{tot}$	–

$$\alpha_j = Nu_j \frac{k_{wf,j}}{d_{H,j}}, \tag{34}$$

where Nu is the local Nusselt number, k_{wf} the fluid thermal conductivity and d_H the hydraulic diameter. The heat transfer correlations used to estimate Nu are described in Appendices A and B. Equation (32) requires a modification when used for plate fin-and-tube heat exchangers, as is shown in Appendix B.

2.5. Heat pump component costing

The costing methodology is based on the authors' previously validated electric heat pump model [11]. Several correlations are updated to better represent the UK market in 2021. Cost correlations for PHEs, electric pumps and the rotary vane compressor are based on data collected for commercially available units on the UK market [50]. For plate fin-and-tube evaporators, the methodology proposed by Guo [74] is employed, which involves breaking down the cost in two parts: a fixed part, assumed to equal the fixed part of the cost of the other heat exchangers (attributed to costs related to design, machining, screw fittings, etc.); and a variable part based on the material cost of copper and the given geometry (as also calculated by Lecompte et al. [75] and Stewart [76]). The cost of the air fans is based on the correlation by Lecompte et al. [75] and the cost of the electronic valves is based on market analysis [77]. To obtain retail prices, additional costs are used to account for miscellaneous hardware (control, meters, etc.), profit margins [78] are and the value-added tax. All cost correlations are listed in Table 2.

2.6. District heating costing

District heating is another sustainable transition pathway that involves producing heat through large-scale, centralised technologies rather than domestic-scale heat pumps or boilers. DH could be suitable in certain areas with high heat demand density. Generation technologies can be either electricity- or hydrogen-based. A comparison to the previously mentioned technologies is performed from a homeowner's perspective, assuming a DH network is already in place. According to the data collected from the Department of Energy and Climate Change for 7 different heat-network schemes in the UK [79], the cost required to connect a house to the DH network is often embedded within the retail price of heat. The average value of the latter for existing schemes in which the operator is responsible for the delivery of heat is close to 0.08 £/kWh. The investment cost to install a heat-interface unit is about £1080 [79] and the annual standing charge for system maintenance is estimated to be £210 [80].

2.7. Definition of performance metrics and inputs

Following technology sizing and costing, the modelled technologies are compared from a homeowner's perspective based on the performance metrics of annual operational cost, annual total cost and levelised cost of heat (LCOH). The annual operational cost involves all annual operating expenses (OPEX) including the maintenance cost, and the annual total cost is the sum of the latter and the equivalent annual capital expenses (CAPEX) [81], as shown in Equation (35):

$$C_{tot,\,ann} = C_{CAPEX,\,ann} + C_{OPEX,\,ann}, \tag{35}$$

where $C_{CAPEX,\,ann}$ is equal to:

$$C_{CAPEX,\,ann} = C_{CAPEX} \frac{r}{1-(1+r)^{-n}}. \tag{36}$$

In Equation (36), r represents the discount rate, n the technology's lifetime and C_{CAPEX} the sum of the investment and installation costs.

The LCOH, which is a measure of the average cost per unit of thermal energy generated over the lifetime of a system, is calculated as shown in the work of Wang et al. [82]:

$$LCOH = \frac{C_{CAPEX} + \sum_{j=1}^{n} C_{OPEX,\,ann}(1+i)^{j-1}(1+r)^{-j}}{\sum_{j=1}^{n} Q_{ann}(1+r)^{-j}}. \tag{37}$$

where i is the inflation rate and Q_{ann} the annual production of thermal energy. The lifetime of the heat pumps, DH and the boiler are assumed to be 20, 20 and 15 years, respectively. The installation costs for the heat pumps and boiler (based on labour fees) are assumed to be £2200 and £1400, respectively [83], and the annual maintenance cost for all technologies except DH is assumed to be £100 [84]. Furthermore, discount and inflation rates are set to 3% [44], and 2.5% [85], respectively.

In the comparisons that follow, the space-heating and hot-water demands of an average UK household are considered. An hourly demand profile is obtained using the normalised profile generated by Sansom [86], which was also used in previous heat-decarbonisation studies [44,87]. The performance of each technology is determined at each hour of the year based on the time-resolved air temperature profile generated for a typical meteorological year for the population centre of the UK by the Photovoltaic Geographical Information System (PVGIS) tool [88]. Heat pumps are sized based on the household's peak annual

Table 3
Energy-system scenarios under investigation to assess the effect on the total system cost towards heating decarbonisation and the system technology mix when domestic heating is decarbonised through electric heat pumps, hydrogen-driven absorption heat pumps or standalone hydrogen boilers.

Scenario	Description
Baseline	• 15 million households switch to net-zero carbon heating • Hydrogen is only produced by electrolysis • Cost of electrolysers as in "Medium" projection from BEIS [92]
High battery cost	• Cost of battery storage is 35% higher than the baseline case
Low electrolyser cost	• Cost of electrolysers as in "Low" projection from BEIS [92]
High electrolyser cost	• Cost of electrolysers as in "High" projection from BEIS [92]
With SMR/ATR	• In addition to electrolysis, hydrogen can also be produced by SMR/ATR in conjunction with CCS
Slower progression	• Only 5 million households switch to net-zero carbon heating

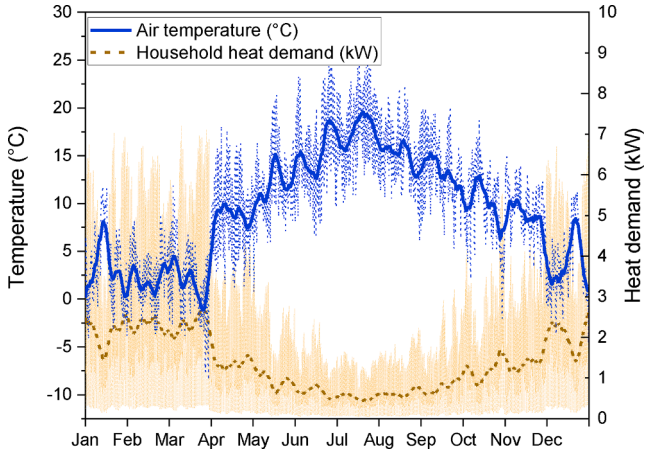

Fig. 5. Hourly and weekly-average values for a snapshot year (2035) of: (i) air-temperature profile based on typical meteorological conditions; and (ii) heat-demand profile of an average UK household.

heat demand, which is a typical sizing method used to ensure that the whole demand is met [89]. Furthermore, the heating technology of each household is assumed to be integrated with a hot-water cylinder, which stores water at the required temperature. The possibility of operating the system flexibly through smart use of the cylinder is not addressed. Therefore, the latter is sized so that the heating technology can charge it in 1 h [90], meaning that it is just large enough to meet all demand.

2.8. Whole-energy system model

An extended version of WeSIM, presented in the work of Pudjianto et al. [43], is used here to assess the system implications associated with each electricity- or hydrogen-driven decarbonisation pathway. WeSIM is a mixed-integer linear programming model that captures the interactions between energy generation, network, storage and demand-side technologies, simultaneously optimising long-term investments in electricity and hydrogen generation and storage assets, as well as short-term technology operation decisions. The objective of the model is to identify country-wide design and operation strategies that lead to the minimum total transition cost to a net-zero electricity system, while: (i) satisfying electricity and heat demand; (ii) ensuring adequate security of supply; (iii) accounting for sufficient volumes of ancillary services; and (iv) meeting the country's carbon emission targets.

In this work, a single-node representation of the UK electricity and heat supply system is assumed without any transmission or interconnection assets (but accounting for the implications of increased demand due to heating electrification on distribution network costs). Investment costs involve electricity generation, electricity storage, electricity distribution, hydrogen generation and hydrogen storage assets. The time resolution is set to 1 h and the model is implemented in the FICO Xpress Optimisation framework [91]. Detailed model formulation can be found in Ref. [43], which was expanded to include hydrogen production technologies such as electrolysis, SMR and ATR. SMR and ATR options include CCS. The associated CO_2 capture rates (90% and 95%, respectively) are chosen based on the projections from the UK Department of Business, Energy and Industrial Strategy (BEIS) [92]. Several different energy system scenarios are investigated, aiming to capture how the system cost and technology mix vary depending on the chosen heating technology and the cost of electricity and hydrogen generation and storage. The investigated scenarios are listed in detail in Table 3.

As stated in the 'Net Zero Strategy' report published by the UK government in 2021 [4], new policies will be set to fully decarbonise the power system by 2035. By the same year, all new heating technologies installed in homes will be either electricity- or hydrogen-driven. Furthermore, policies will be put in place for heat pump rollout to be accelerated with an aim to install 600 000 heat pumps per year from 2021 until 2035. Based on these targets, all explored scenarios focus on 2035 as a snapshot year and assume that the electricity and hydrogen supply should involve net-zero carbon emissions. In the baseline scenario, it is assumed that 15 million households (about 60% of the country's total) switch from their current heating technology to either an electric heat pump, a hydrogen-driven absorption heat pump or a standalone hydrogen boiler. The design of the energy system is optimised so that the heat provided to the households that switch is carbon neutral. To achieve this target, the model includes the option to invest in carbon-negative technologies such as bioenergy with CCS (BECCS). Therefore, even though the model allows some carbon emissions from gas-fired power generation, SMR and ATR, these emissions can be offset to achieve net-zero emissions. The cost-optimal capacity of BECCS is determined by the model depending on the operation of unabated thermal generation as well as on the utilisation of SMR and ATR capacities that are found to be optimal from the system's perspective. Large-scale electricity storage is assumed to take the form of lithium-ion batteries. In all scenarios except one, hydrogen is generated by electrolysis.

The assumed costs of electricity generation technologies are based on BEIS projections of electricity generation costs [93]. Similarly, the cost and technical parameters of hydrogen production technologies are selected to be in line with the recent hydrogen production cost projections published by BEIS [92].

3. Results and discussion

In this section, the results of the technoeconomic and whole-energy system comparisons of electricity- and hydrogen-driven technologies are presented. The performances of the electric and absorption heat pumps are first analysed for various heat-source and -sink temperatures. This is followed by an assessment of the competitiveness of the two systems along with that of a standalone hydrogen boiler and DH for various electricity, hydrogen and DH price scenarios. Lastly, the technologies are compared in terms of their implications for national-scale, whole-energy system design and overall transition cost.

In all comparisons, a 10% reduction in the total UK heat demand is assumed in 2035 compared to current levels, so as to account for energy-efficiency measures and behavioural changes over time. This is in line with estimates provided in the Sixth Carbon Budget report of the CCC [94]. The hourly and weekly-averaged heat demand and air-temperature profiles are presented in Fig. 5. As shown, the value of the peak demand is equal to about 7 kW_{th}.

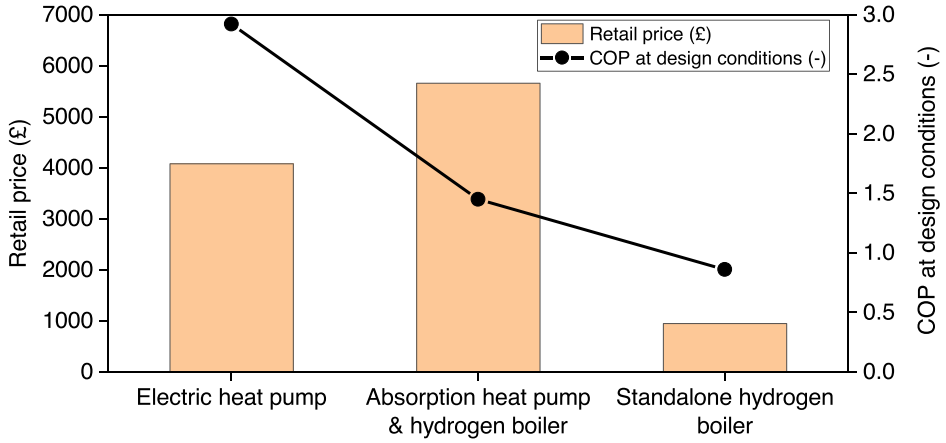

Fig. 6. Retail price and COP at design conditions (hot-water demand temperature of 55 °C and air temperature of 7 °C) of electric heat pump, absorption heat pump driven by heat from a hydrogen boiler, and standalone hydrogen boiler for an average UK household. Note: the COP in the case of the hydrogen boiler refers to its efficiency (i.e., heat output over fuel input).

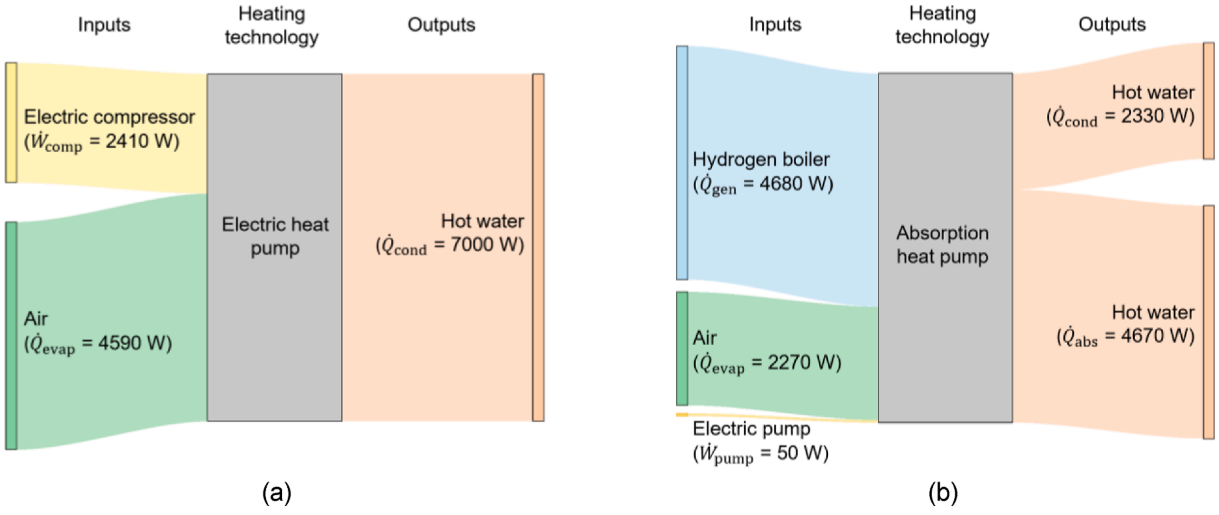

Fig. 7. Sankey diagrams depicting energy flows at nominal heating capacity (7 kW_{th}), with a hot-water demand temperature of 55 °C and an air temperature of 7 °C for: (a) electric heat pump; and (b) absorption heat pump driven by heat from a hydrogen boiler.

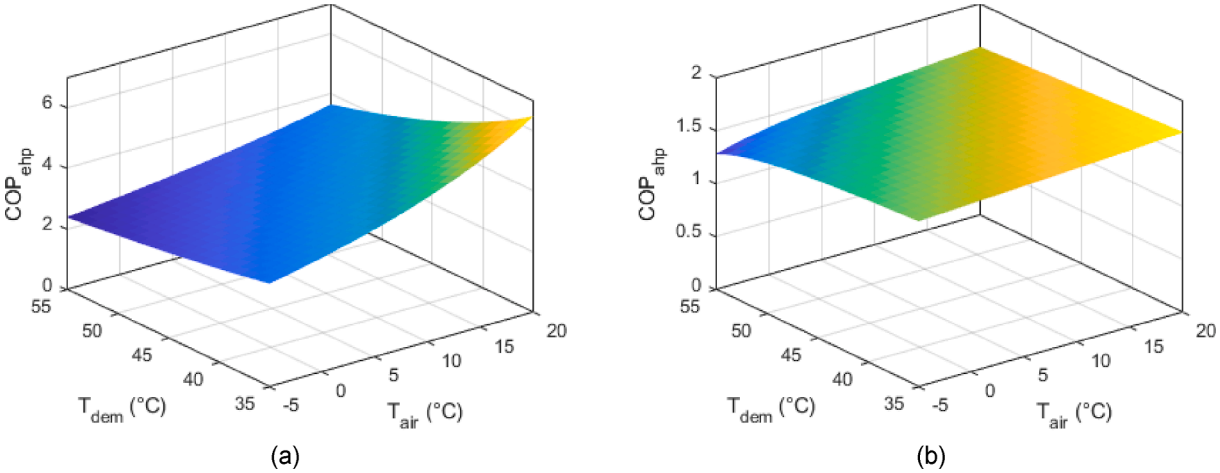

Fig. 8. COP as a function of air and hot-water demand temperatures for: (a) electric heat pump; and (b) absorption heat pump. Note: the COP definitions are different (see Sections 2.1 and 2.3).

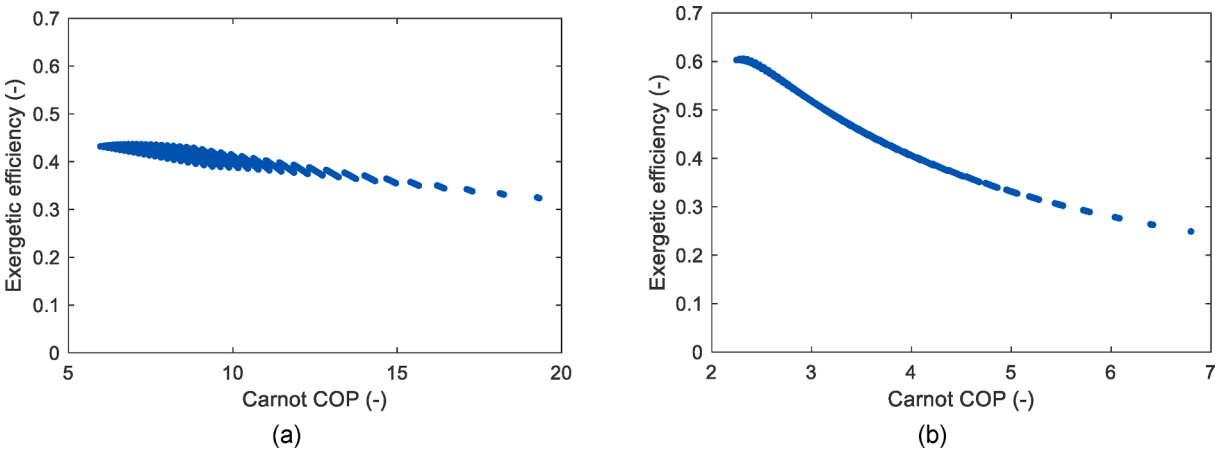

Fig. 9. Exergetic efficiency as a function of Carnot COP for: (a) electric heat pump; and (b) absorption heat pump, when varying the air temperature between −5 °C and 20 °C and the hot-water demand temperature between 35 °C and 55 °C.

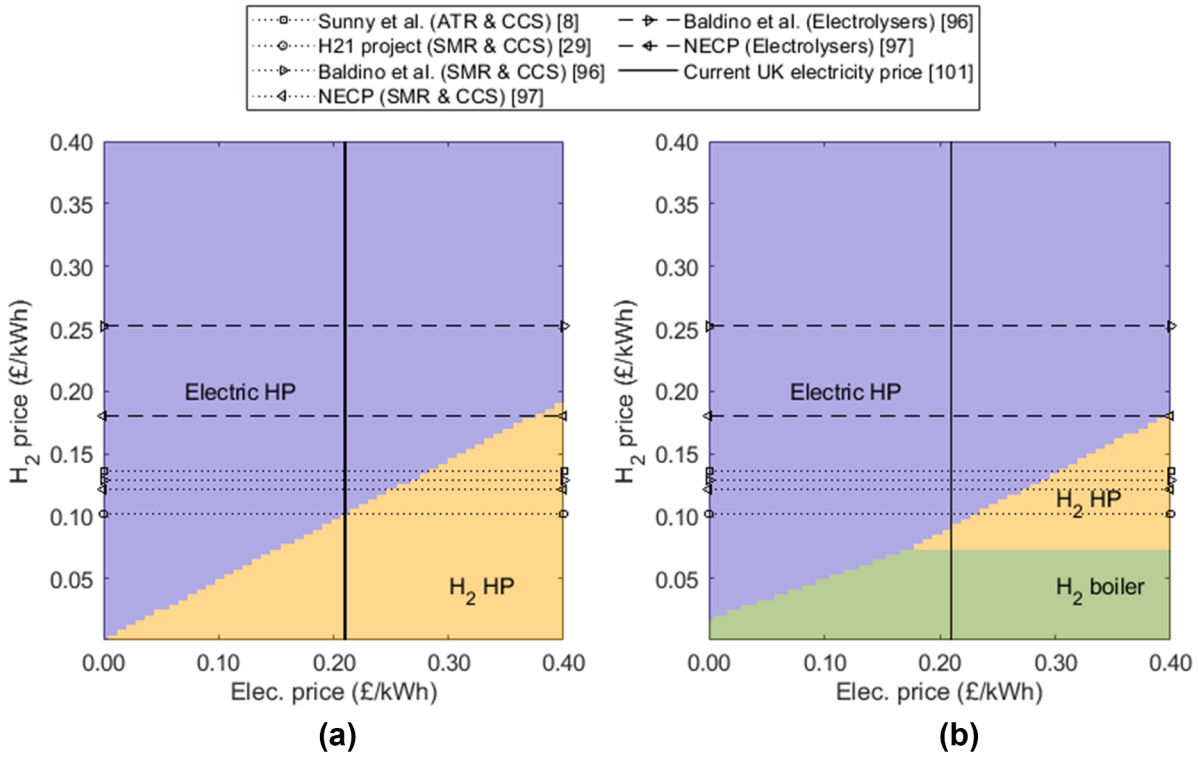

Fig. 10. Comparison of electric heat pump, hydrogen-driven absorption heat pump and standalone hydrogen boiler for different electricity and hydrogen household prices based on: (a) annual operational cost; and (b) annual total (investment, operational and maintenance) cost. Different colours indicate which of the three technologies has the lowest cost for a given combination of electricity and hydrogen prices. Horizontal and vertical lines represent the estimated retail prices of carbon–neutral hydrogen from different sources and the current electricity price in the UK, respectively.

3.1. Technoeconomic analysis at design point

The component sizing and costing exercise of domestic technologies is conducted based on a hot-water demand temperature of 55 °C and an air temperature of 7 °C, which are standard conditions used by manufacturers in the UK to report heat pump performance [95]. The retail price and efficiency at standard conditions of the electric heat pump, the hydrogen-driven absorption heat pump and the hydrogen boiler are shown in Fig. 6. The Sankey diagrams in Fig. 7 show the energy flows when the electric and absorption heat pumps are operated at their nominal heating capacity (7 kW_{th}).

The COP of the electric heat pump at standard conditions is found to be 2.92, which is within 3% of the value of an average R32 heat pump currently on the UK market [50]. Its retail price is estimated to be £4060 (specific price: 580 £/kW_{th}), again in line with commercially available units [50]. The hydrogen boiler efficiency is calculated to be 86%. Based on the authors' analysis of commercially available gas boilers [50], its price for an average UK household is assumed to be £980. Lastly, the COP of the absorption heat pump at the standard conditions is found to be 1.45, which is in line with values found in literature for similar size and fluid systems [30,33,41]. Its price is calculated to be £4680 and since it is driven by heat from a hydrogen boiler, the total system price is equal to £5660 (specific price: 810 £/kW_{th}).

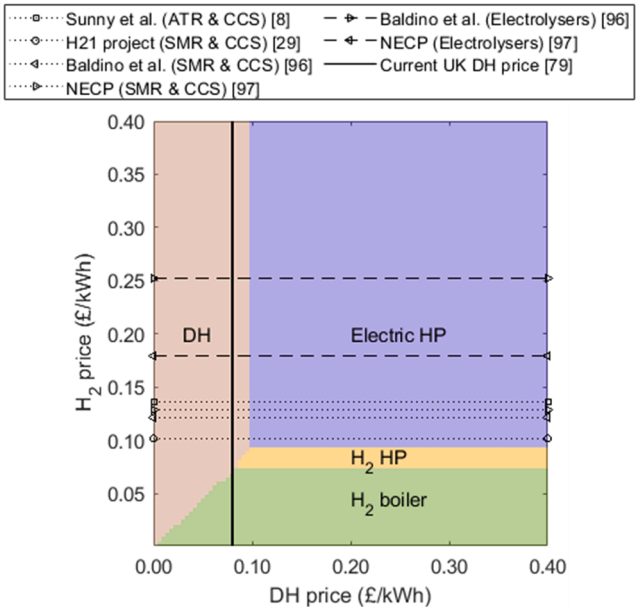

Fig. 11. Comparison of electric heat pump, hydrogen-driven absorption heat pump, standalone hydrogen boiler and DH for different hydrogen and DH household prices based on total annual (investment, operational and maintenance) cost. Different colours show which of the four options has the lowest cost for a given combination of electricity and hydrogen prices. Horizontal and vertical lines represent the estimated retail prices of carbon–neutral hydrogen from different sources and the current average DH price in the UK, respectively. The electricity price is fixed at the current UK value (0.21 £/kWh).

3.2. Heat pump performance at different heat-source and heat-sink conditions

The COP of the electric and absorption heat pumps is determined for a range of demand and source temperatures, as shown in Fig. 8. The analysis assumes a fixed 5-K pinch-point temperature difference between the working fluid and heat sources/sinks. The air temperature is varied between −10 °C and 20 °C, capturing the variations in system performance during different UK seasons. The demand temperature is varied between 35 °C and 55 °C, covering the range of applications from low-temperature underfloor space heating to domestic hot water provision.

For a demand temperature of 55 °C, the COP of the electric heat pump varies between 2.4 and 3.7 for different weather conditions. The electric heat pump performs especially well under low demand-temperature conditions, with the COP varying between 3.4 and 6.3 for a demand temperature of 35 °C. The absorption heat pump provides more consistent COP values over the considered temperature ranges, varying between 1.3 and 1.7 over most of the tested range. A deterioration in performance is observed when the air temperature is low (close to −5 °C) and the demand temperature is 55 °C.

The exergetic efficiency of the two technologies, which is a measure that enables a thermodynamic assessment of their effectiveness, is also investigated. The latter is plotted as a function of Carnot COP for all temperature combinations in Fig. 9. The absorption heat pump is associated with a higher exergetic efficiency for most of examined working conditions. In detail, the exergetic efficiency is shown to be higher than 0.5 for Carnot COP values lower than 3, but as the latter increases to more than 6, the exergetic efficiency drops below 0.3. The electric heat pump exergetic efficiency has a lower dependence on the Carnot COP (as the cycle involves one heat source and one heat sink, compared to two heat sources and two heat sinks in an absorption heat pump), varying from about 0.35 to 0.45 for the tested conditions.

It is worth noting that the analysis of the COP and exergetic efficiency of electric and absorption heat pumps shown in Figs. 8 and 9 does not account for the fact that the hydrogen boiler that supplies heat to the absorption heat pump is also associated with some energy (i.e., heat) loss and exergy destruction. Furthermore, the competitiveness of the different options is not only a function of their thermodynamic performance but also depends on the prices of electricity and hydrogen. This means that a complete comparison requires one to analyse the combined technoeconomic (technical and economic) potential of the possible options for different fuel price scenarios, which is presented in the next section.

3.3. Technoeconomic comparison for different fuel price scenarios

The annual operational and total costs associated with the electric heat pump, hydrogen-driven absorption heat pump and hydrogen boiler are estimated based on different electricity- and hydrogen-price scenarios as described in Section 2.7 and are compared in Fig. 10. Different colours indicate which of the three technologies has the lowest annual operational cost (Fig. 10(a)) or total cost (Fig. 10(b)) for a given combination of electricity and hydrogen prices.

The predicted prices of hydrogen delivered to homes show large variations across the literature. Northern Gas Networks predict in the "H21 project" report [29] that hydrogen could be produced at a wholesale price of 0.051 £/kWh including all costs associated with SMR, CCS, hydrogen storage and gas-network reinforcement. Distribution and operating costs are estimated to account for about 25% each, which means that the total price for domestic consumers could potentially be close to 0.102 £/kWh. Furthermore, Sunny et al. [8] estimate that, excluding distribution-related and other charges, carbon–neutral hydrogen could be supplied at 0.068 £/kWh. This price includes generation via ATR and biomass gasification with CCS, underground hydrogen storage and gas-network reinforcement. Similar to Northern Gas Networks, the authors estimate distribution-related charges to be 25%. Assuming the same portion of other operating costs (25%), this wholesale price translates to a retail price of 0.136 £/kWh. The prediction from Sunny et al. [8] aligns well with the prediction in the white paper of Baldino et al. [96], who estimated a heat supply price of hydrogen close to 0.066 £/kWh when produced by SMR and CCS (which, assuming 25% for the distribution and 25% for other costs, translates to a retail price of 0.132 £/kWh). Lastly, in a study conducted by the Trinomics and LBST consultancies [97] to analyse the role of hydrogen in the National Energy and Climate Plans (NECP), the authors estimate that, in the UK, if hydrogen is produced by SMR and CCS, it could be delivered at a cost of 0.061 £/kWh, which translates to retail price of 0.122 £/kWh.

Hydrogen produced using renewable electricity sources and electrolysis rather than methane reforming and CCS is expected to be more expensive. Baldino et al. [96] estimate that hydrogen produced by electrolysis would cost about 0.126 £/kWh, which translates to a retail price of about 0.252 £/kWh. In the study of Trinomics and LBST [97], the expected delivery cost in the case of electrolysis is estimated to be 0.09 £/kWh, which means a price of 0.18 £/kWh for domestic consumers. At this price, it is unlikely for hydrogen to be competitive to electricity. In fact, the Fuel Cells and Hydrogen Joint Undertaking has set a goal to reach a retail price of renewably produced hydrogen of 0.11–0.15 £/kWh by 2025 [98,99], while it is stated in the strategic research and innovation agenda of the Clean Hydrogen for Europe partnership [100] that renewably produced hydrogen should be produced at a cost below 0.065 £/kWh by 2030 to become competitive. The estimated retail price of carbon–neutral hydrogen from different sources and the current UK average electricity price (0.21 £/kWh) [101] are shown as lines in Fig. 10.

The price ranges used for the axes of Fig. 10 for both electricity and hydrogen (0–0.40 £/kWh) are chosen to capture a very wide range of price scenarios, including the extreme cases in which the electricity or hydrogen prices become extremely low (close to 0 £/kWh) or extremely

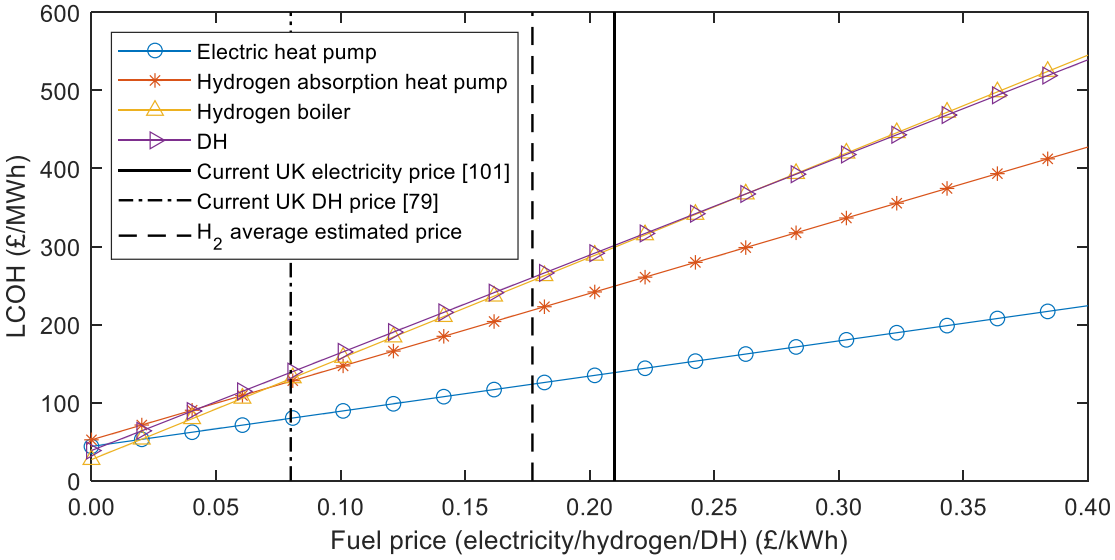

Fig. 12. Levelised cost of heat (LCOH) for the electric heat pump, hydrogen-driven absorption heat pump, standalone hydrogen boiler and DH for different electricity, hydrogen and DH household prices.

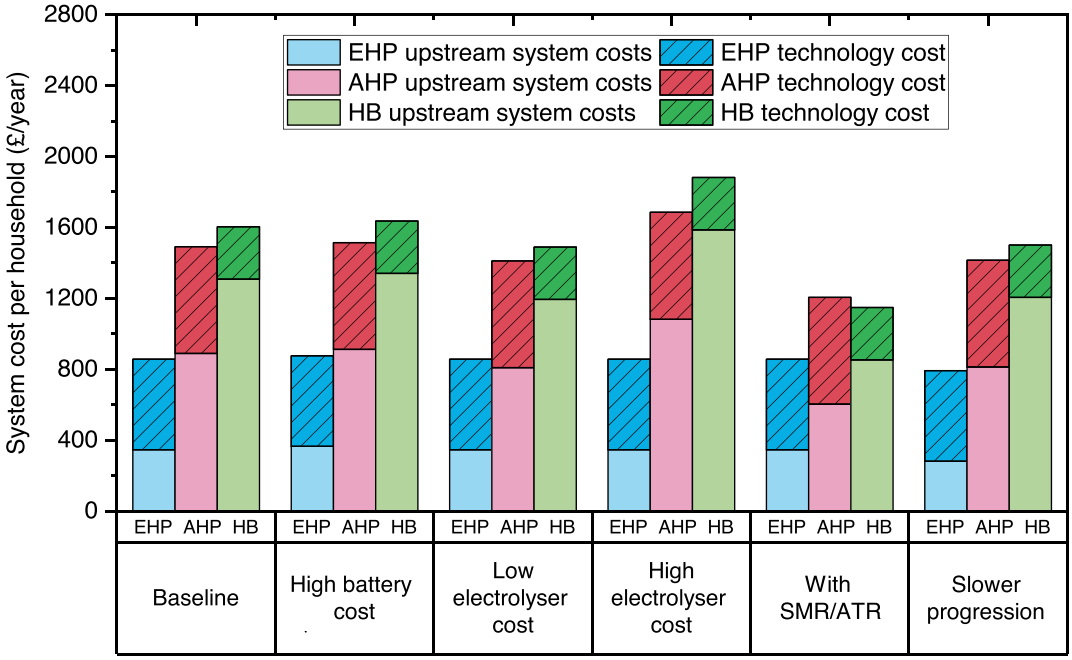

Fig. 13. Total system transition cost to decarbonise the UK domestic heating sector by 2035 when heat is delivered through: (i) electric heat pumps (EHPs); (ii) hydrogen-driven absorption heat pumps (AHPs); or (iii) standalone hydrogen boilers (HBs), for six investigated scenarios. The total system cost is broken down into two parts: (i) the upstream system costs, which include all electricity and hydrogen generation and storage costs associated with carbon–neutral heating provision; and (ii) the technology cost, which includes the annualised investment, installation and maintenance cost associated with the heating technology.

high (double the current values or expected estimates, respectively).

Electric heat pumps cover the largest areas of Fig. 10(a) and (b), showing that they are currently one of the most competitive domestic technologies under various electricity and hydrogen price scenarios. Given that the current average electricity price in the UK is 0.21 £/kWh [101], the annual operational cost (Fig. 10(a)) associated with a hydrogen-driven absorption heat pump is lower than that of the electric heat pump for hydrogen prices below 0.10 £/kWh. When considering only the operational costs, the hydrogen boiler is always less cost-efficient than the electric and absorption heat pumps under all price scenarios, and therefore it does not appear in Fig. 10(a).

Since the investment cost of the absorption heat pump system is slightly higher than that of the electric heat pump, the competitiveness of the latter marginally improves when looking at the annual total cost (Fig. 10(b)). If hydrogen is produced by SMR or ATR in conjunction with CCS, and thus the hydrogen price is close to the values predicted by Refs. [8,29,96,97], hydrogen technologies start to be competitive. At the current UK electricity price, absorption heat pumps are competitive compared to electric systems for hydrogen prices below about 0.09 £/kWh, and hydrogen boilers become favourable relative to absorption heat pumps for prices below 0.07 £/kWh. If hydrogen is produced by electrolysis, given the current estimates for the costs of the required equipment, the associated predicted retail price is much higher (0.18–0.25 £/kWh), making electric heat pumps the most cost-effective

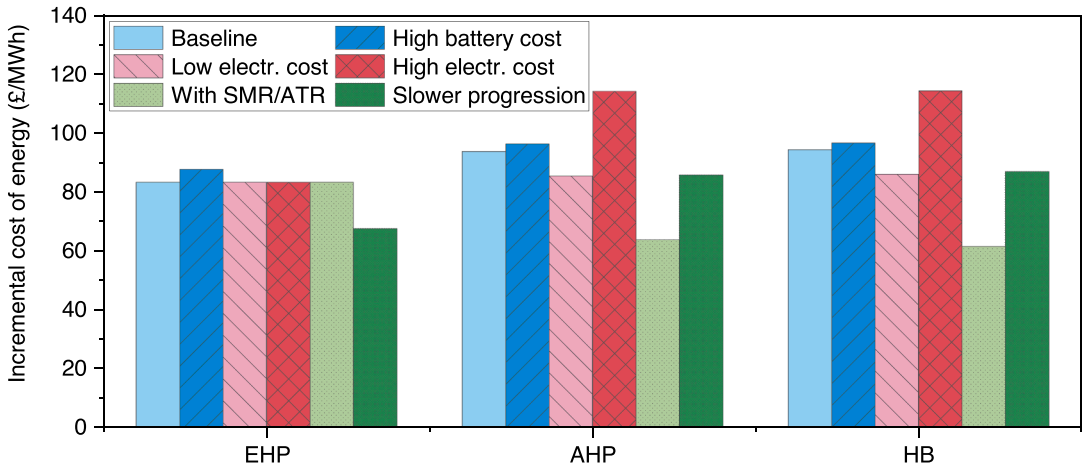

Fig. 14. Incremental cost of energy in the UK in 2035 when domestic heating is decarbonised through: (i) electric heat pumps (EHPs); (ii) hydrogen-driven absorption heat pumps (AHPs); or (iii) standalone hydrogen boilers (HBs), for six investigated scenarios. In the case of electric heat pumps, this represents the total upstream electricity generation and storage costs divided by the total heat-related electricity demand, and in the case of hydrogen technologies, it represents the total upstream hydrogen generation and storage costs divided by the total heat-related hydrogen demand.

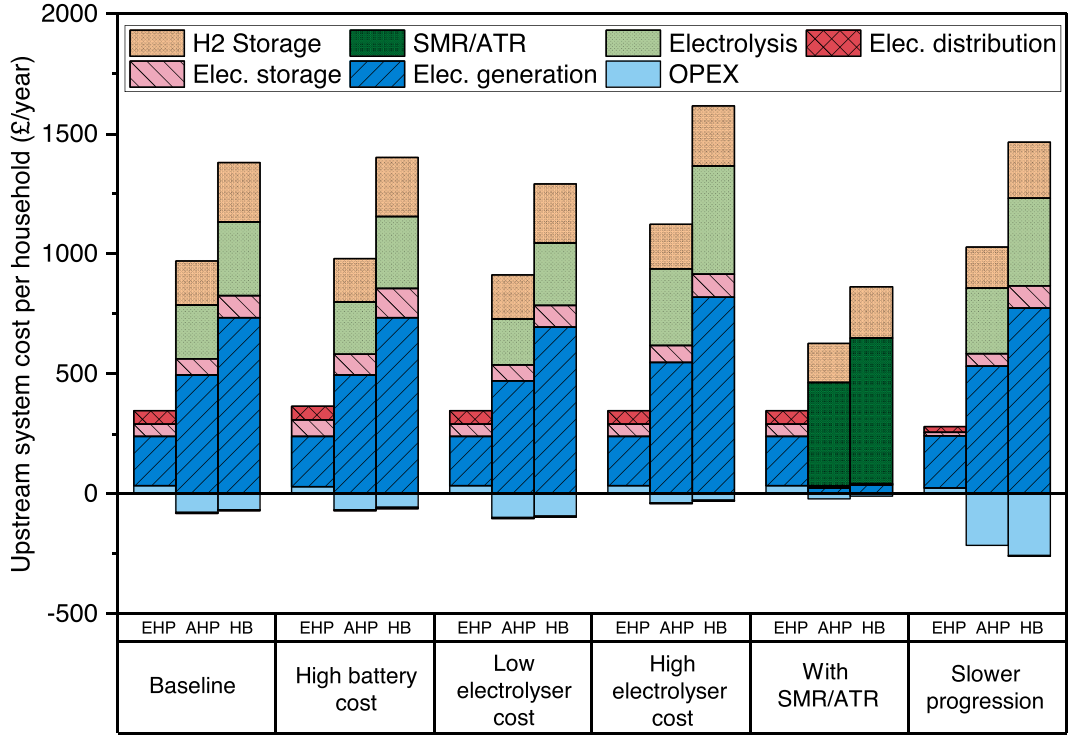

Fig. 15. Components of upstream system costs in the UK in 2035 when domestic heating is decarbonised through: (i) electric heat pumps (EHPs); (ii) hydrogen-driven absorption heat pumps (AHPs); or (iii) standalone hydrogen boilers (HBs), for six investigated scenarios.

option. Therefore, provided that electricity prices do not drastically drop in the future, the competitiveness of hydrogen boilers and hydrogen-driven heat pumps will be determined by the ability to produce hydrogen in a cost-effective way.

3.4. Comparison to district heating

Fig. 11 shows the comparison of DH (when this is an available option for homeowners) against the electricity- and hydrogen-driven options based on total annual cost for a fixed electricity price at the current UK value of 0.21 £/kWh and for various hydrogen and DH prices.

As shown in Fig. 11, DH systems can be the most economical heating option for domestic consumers (in locations where this option is available) if heat can be supplied at a price lower than about 0.10 £/kWh. At the average price of heat of existing UK DH schemes (0.08 £/kWh) [79] and given the current electricity price (0.21 £/kWh), DH seems to be the best choice for households with this option. However, most existing schemes are based on gas-fired CHP systems, which means that higher investments may be required in the future for the heat delivered from DH systems to be net-zero carbon. Furthermore, installing DH networks in less suitable (e.g., rural) regions could cause a further increase in the price of heat. If the latter is higher than 0.10 £/kWh, all other heating options come into discussion and the choice of the most cost-effective one is highly dependent on the price of hydrogen, which is highly uncertain.

The LCOH associated with the different technologies is shown in

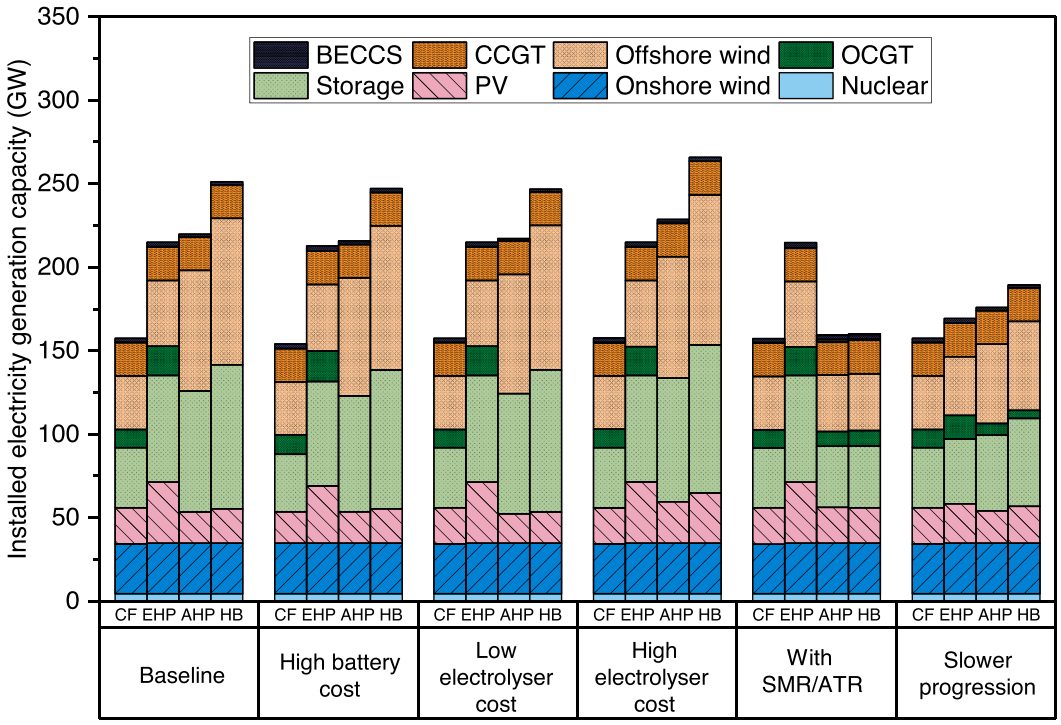

Fig. 16. UK electricity technology mix in 2035 when domestic heating is not decarbonised (counterfactual (CF)) case) and when it is decarbonised through: (i) electric heat pumps (EHPs); (ii) hydrogen-driven absorption heat pumps (AHBs); or (iii) standalone hydrogen boilers (HBs), for six investigated scenarios.

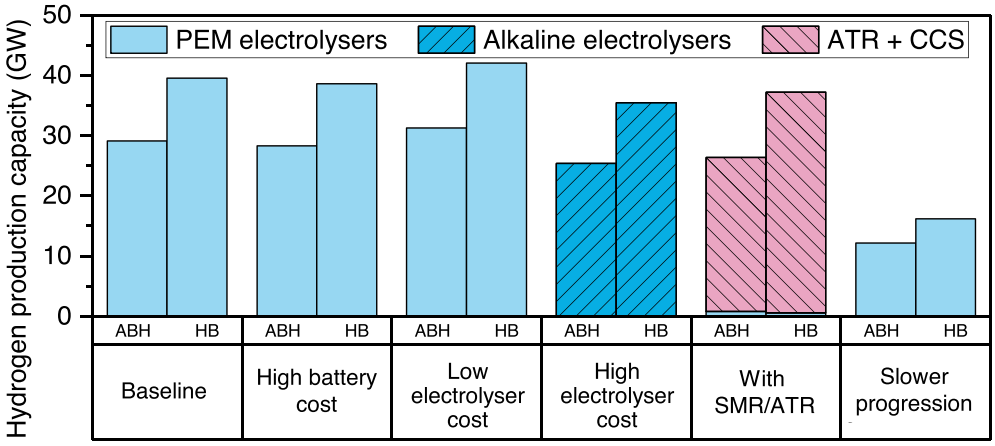

Fig. 17. UK hydrogen production capacity in 2035 when domestic heating is decarbonised through: (i) hydrogen-driven absorption heat pumps (AHPs); or (ii) standalone hydrogen boilers (HBs), for six investigated scenarios.

Fig. 12. Vertical lines are used to indicate the current UK electricity price [101], DH price [79], and estimated H_2 price (average value from the reported sources). The LCOH of each of these options has a different relationship with fuel price. Hydrogen boilers and DH, which exhibit lower efficiencies (and thus higher operating costs) compared to electric or absorption heat pumps, are shown to have low LCOH at low hydrogen or DH heating prices, but with increasing prices, these two heating options are associated with the highest LCOH. The LCOH of electric heat pumps shows a smaller dependence on the price of electricity due to their high operating performance compared to the other options, which means it is less affected by the uncertainty in future fuel prices, and also less sensitive to fuel price variations.

Government incentives would significantly affect the comparison of technologies shown in Figs. 10-12. Intervention through subsidies, carbon taxes or even bans on certain technologies could be used to encourage the uptake of technologies that are optimal from a whole-system perspective. It is therefore important to assess the implications of each of the investigated technology options to the energy system.

3.5. National energy-system effects in the UK

The thermodynamic and component-costing models of the heating technologies were used to provide inputs to the WeSIM whole-energy system model to investigate the effects of the uptake of the different options on the energy system transition cost and technology mix. This involves integrating the COP and air-temperature relationships described in Section 3.2 within WeSIM and using the same investment costs, heat demand profile and air temperature profile as those used for the comparison conducted from the homeowner's perspective in Sections 3.3 and 3.4. In all scenarios, heating decarbonisation is assumed to take place exclusively through one of the three technology options in each case (electric heat pump, hydrogen-driven absorption heat pump or

standalone hydrogen boiler), thus capturing the full range of different energy-system effects. As this is a single-node model, DH is not investigated.

Fig. 13 shows the total system cost per household to provide net-zero carbon heating by 2035 for the six investigated system scenarios listed in Table 3 in Section 2.8. The total annual heating cost per household is broken down into two parts: (i) the upstream system costs obtained from the whole-energy system model, including all upstream electricity and hydrogen generation and storage costs associated with carbon–neutral heating provision; and (ii) the technology cost, which includes the annualised investment, installation and maintenance cost associated with the heating technology. To obtain the upstream costs, the incremental system cost of supplying electricity and hydrogen for heating is quantified as the difference between total system cost in a scenario with net-zero carbon heating and a counterfactual scenario with no net-zero carbon heating. This difference is then divided by the number of households that switch to carbon neutral heating, and the resulting upstream costs are presented in Fig. 13. System cost of net-zero carbon heating is also quantified as average unit cost of electricity or hydrogen delivered to households, by dividing the incremental system cost with the total heat-related electricity or hydrogen demand, respectively. The resulting energy costs are shown in Fig. 14.

As shown in Fig. 13, electric heat pumps involve the lowest total system cost per household in all investigated scenarios. In the baseline scenario, which involves 15 million households switching to net-zero carbon heating by 2035, the upstream costs associated with investments in electricity production, storage and operation of these assets for the case of electric heat pumps are about 350 £/year. If heat is provided through hydrogen produced by electrolysis (assumption of the baseline scenario), hydrogen production and storage costs largely depend on the heating technology due to variations in the required volume of hydrogen (890 £/year for absorption heat pump vs. 1310 £/year for hydrogen boiler). Hydrogen boilers are cheaper than both electric and absorption heat pumps, however, when accounting for both the upstream supply and technology costs, electric heat pumps are the most cost-effective option. The latter technologies are associated with a total system cost per household equal to 860 £/year, while absorption heat pumps are shown to be slightly better than hydrogen boilers (1490 £/year compared to 1600 £/year). Furthermore, in the baseline scenario, the incremental cost of electricity is slightly lower than that of hydrogen (83 £/MWh compared to 94 £/kWh – Fig. 14), which compounds the effect of lower energy requirements by electric heat pumps than the two hydrogen options.

The five additional scenarios are used to show how results change with variation in some of the energy-system model assumptions. When the price of electricity storage is higher than in the baseline case, there is a slight increase in upstream storage costs associated with electric heat pumps, but this is insignificant when comparing the technologies. Low and high electrolyser cost assumptions show significant effect on the hydrogen upstream costs (Fig. 13) and cost of hydrogen (Fig. 14), but in both cases electric heat pumps are still characterised by significantly lower total system costs.

When SMR/ATR in conjunction with CCS are assumed to be an available option for hydrogen production, hydrogen production costs are significantly lower. It is important to note that due to the imperfect carbon capture rate (assumed as 90% for SMR and 95% for ATR) the reformation technology options for hydrogen production are made possible by investing in NETs, such as BECCS, although it is noted that the capacity of BECCS plants required to offset SMR and ATR carbon emissions in the model results was an order of magnitude lower than the capacity required to offset emissions from unabated gas generation. Although electric heat pumps are still the most competitive option even in this scenario, the difference between the total system cost of the electrification scenario and the hydrogen scenarios is reduced by more than 50%. Another interesting observation is that, when hydrogen is produced by SMR/ATR with CCS, the total system cost associated with hydrogen boilers becomes lower than that of absorption heat pumps. This fits well with the technoeconomic comparison of technologies in Sections 3.3 and 3.4, demonstrating that the lower the cost of hydrogen production, the more competitive hydrogen boilers are compared to hydrogen-driven absorption heat pumps. Lastly, a reduction in the number of households that switch to net-zero carbon heating by 2035 (5 million in the "slower progression" scenario compared to 15 million in the baseline) leads to reduced system costs per household for all heating technologies, as the lower volume of heat demand is integrated more cost-effectively with the baseline demand of the power system.

The breakdown of the upstream system costs is shown in Fig. 15. Key components include electricity system OPEX, generation, storage and distribution assets, electrolyser and reformation capacity and hydrogen storage. Most upstream costs in the case of electric heat pumps are associated with increased investment in renewable generation, with some increase driven by higher investment in distribution network and in battery storage. The investment cost of generation capacity increases further in the case of hydrogen heating pathways, also accompanied by sizeable investments into electrolyser (or reformation) and hydrogen storage capacity. Furthermore, as the percentage of hydrogen in distribution networks is currently limited due to safety aspects [19,20], additional costs for transportation in the future may drive the total costs associated with hydrogen pathways even higher than those shown in Fig. 15. In the UK, more than 60% of iron gas pipelines have already been replaced with polyethylene pipes during the Iron Mains Risk Reduction Programme. As stated in Britain's hydrogen network plan [19], these will eventually allow 100% hydrogen to be transported, but further feasibility tests will be required.

The national electricity generation capacity breakdown is shown in Fig. 16 for different scenarios. The counterfactual net-zero carbon power system is based on a mix of nuclear and variable renewable capacity (including onshore and offshore wind and solar PV), with some legacy gas combined cycle gas-turbine (CCGT) generation and a small volume of BECCS to compensate for the carbon impact of gas-fired generation. The electricity demand increase in the electric heat pump scenario, leads to the addition of more renewable generation plants as well as an increased amount of battery storage and peaking open cycle gas-turbine (OCGT) plants to cope with the increase in peak demand. In scenarios where hydrogen is supplied through electrolysers, it is necessary to build even more renewable generation capacity. If hydrogen can be supplied through reformation technologies that use natural gas (SMR/ATR), the resulting impact on the power system is minimal compared to the counterfactual.

Lastly, the breakdown of hydrogen production capacity across different scenarios is shown in Fig. 17. Except in the "Slower progression" scenario which involves a smaller number of households with net-zero carbon heating, the required hydrogen production capacity across different scenarios is between 25 and 31 GW in the case of hydrogen-driven heat pumps, and between 35 and 42 GW in the case of hydrogen boilers. The preferred type of electrolyser technology is proton exchange membrane (PEM) except in the scenario with higher electrolyser costs when alkaline electrolysers are more cost-effective. In case with SMR and ATR, most of the production capacity is provided by ATR with CCS.

Overall, the results of this section demonstrate that, although the cost of electrifying heating is significant, given the rapid reduction in the cost of renewable generation technologies such as wind and solar PV in recent years, electrification currently appears to be the lower-cost pathway towards heating decarbonisation in the UK. In the case of a hydrogen-based decarbonisation pathway, both hydrogen boilers and hydrogen-driven heat pumps could be competitive. The possibility to inject hydrogen in the existing gas network could be an effective option in the UK; however, producing hydrogen remains costly. The integration of reformation systems in conjunction with CCS in the energy technology mix shows to have a significant role to play in bringing down costs associated with hydrogen pathways.

4. Conclusions

Several pathways based on electricity and hydrogen are currently being discussed in the context of domestic sector heating decarbonisation. In this paper, comprehensive thermodynamic and component-costing models of a domestic electric heat pump, an ammonia-water absorption heat pump driven by heat from a hydrogen boiler and a standalone hydrogen boiler were developed. Using an average UK household as a focal case study, the technologies were sized and costed using a framework of consistent modelling methodology and assumptions. Along with the option of DH, the competitiveness of different technologies was first assessed for various electricity, hydrogen and DH prices from a homeowner's perspective. Then, the developed models were used to provide inputs to WeSIM, a whole-energy system model of the UK, which was used to investigate the effects of the uptake of these technologies on the energy system transition cost and technology mix.

The electric heat pump, for which components were chosen to align with domestic units currently available on the UK market, has a COP of 2.92 at design conditions and a specific price of 580 £/kW_{th}. The hydrogen-driven absorption heat pump, on the other hand, has a COP at design conditions of 1.45, which is in line with values found in the literature, and a specific price of 810 £/kW_{th}. The thermodynamic comparison of the two systems for various working conditions is insightful, but the competitiveness of the two systems largely depends on the relative prices of electricity and hydrogen.

From a homeowner's perspective, electric heat pumps were found to be the most competitive technology in most electricity and hydrogen price scenarios. This is in line with the vision that although hydrogen could be a competitive solution for sectors such as heavy transport, hard-to-abate industrial segments, long-term energy storage or production of synthetic fuels, electrification appears to be more promising for the decarbonisation of residential heat demand. At the current UK electricity price for domestic consumers (0.21 £/kWh), absorption heat pumps and hydrogen boilers become competitive for hydrogen prices below about 0.09 £/kWh. Therefore, if electricity prices do not significantly drop in the future, the competitiveness of hydrogen technologies will depend on the ability to produce hydrogen cost-effectively. In the case that DH is an additional option for homeowners, it was shown to be the best option if heat can be supplied at a price lower than 0.10 £/kWh. Currently in the UK, the average value of the latter for existing schemes is 0.08 £/kWh, however, this could be higher in the future as higher investments may be required for the heat delivered from DH systems to be net-zero carbon. In terms of LCOH, that of electric heat pumps was found to be 0.14 £/kWh at the current UK electricity price, which is lower than that of hydrogen technologies (0.15–0.35 £/kWh) for the hydrogen price estimates provided in literature.

The different electricity and hydrogen-driven heating options were also compared from a national, whole-energy-system perspective. The total system cost per household associated with electric heat pumps was shown to be in the range 790–880 £/year for different system scenarios, making it the lowest-cost decarbonisation pathway. Upstream effects in this case will involve increased renewable electricity generation and storage. Assuming that hydrogen is produced by electrolysis, the total system cost associated with hydrogen boilers or absorption heat pumps was significantly higher, at 1410–1880 £/year. It was shown that this scenario requires even more renewable electricity generation capacity than the case of electric heat pumps. However, if hydrogen can be produced cost effectively by ATR with CCS, the system cost drops down to 1150 £/year, reducing the gap between the two technologies. Furthermore, it was shown that when considering total system transition costs, hydrogen-driven absorption heat pumps are a competitive alternative to hydrogen boilers in all hydrogen-pathway scenarios.

Overall, this paper provides insights into the potential of currently proposed domestic heating options and into the key technoeconomic factors that influence their competitiveness in the context of heating decarbonisation. The comparison from both a homeowner's and a whole-energy-system perspective provides evidence to support both technology advancement and energy policy.

CRediT authorship contribution statement

Andreas V. Olympios: Conceptualization, Formal analysis, Methodology, Software, Writing – original draft, Writing – review & editing. **Marko Aunedi:** Formal analysis, Methodology, Software, Writing – original draft, Writing – review & editing. **Matthias Mersch:** Investigation, Methodology, Software, Writing – review & editing. **Aniruddh Krishnaswamy:** Formal analysis, Investigation, Software, Writing – original draft. **Corinne Stollery:** Formal analysis, Investigation, Software, Writing – original draft. **Antonio M. Pantaleo:** Conceptualization, Methodology, Writing – review & editing, Supervision. **Paul Sapin:** Conceptualization, Software, Writing – review & editing, Supervision. **Goran Strbac:** Supervision, Resources, Project administration. **Christos N. Markides:** Conceptualization, Methodology, Project administration, Resources, Supervision, Writing – review & editing.

Declaration of Competing Interest

The authors declare that they have no known competing financial interests or personal relationships that could have appeared to influence the work reported in this paper.

Acknowledgments

This work was supported by the UK Engineering and Physical Sciences Research Council (EPSRC) [grant numbers EP/V042149/1, and EP/R045518/1], and the UK Natural Environment Research Council (NERC) [grant number NE/L002515/1]. The authors would also like to acknowledge the Science and Solutions for a Changing Planet (SSCP) Doctoral Training Partnership (DTP). Data supporting this publication can be obtained on request from cep-lab@imperial.ac.uk. For the purpose of Open Access, the authors have applied a CC BY public copyright licence to any Author Accepted Manuscript version arising from this submission.

Appendix A. . Plate heat exchanger heat transfer correlations

The geometrical parameters of PHEs are based on small liquid-to-liquid units currently available in the UK market [102,103] and are shown in Table A.1. Based on these, the number of plates that are required to achieve the required heat transfer of each heat exchanger is identified.

For PHEs, the hydraulic diameter is determined based on Equation (A.1) proposed by Mounier et al. [104]:

$$d_H = 2\delta_{chan}\left[\frac{1}{6}\left(1+\sqrt{1+\left(\frac{\pi\delta_{chan}}{2\Lambda}\right)^2}+4\sqrt{1+\left(\frac{\pi\delta_{chan}}{2\sqrt{2}\Lambda}\right)^2}\right)\right]^{-1}. \quad (A.1)$$

Table A1
Main geometrical parameters used in PHE models.

Parameter	Description	Value	Ref.
w_{chan}	channel width	74 mm	[102]
l_{chan}	channel length	210 mm	[102]
δ_w	plate thickness	0.2 mm	[102]
δ_{chan}	plate spacing	1.9 mm	[102]
β	chevron angle	30°	[103]
Λ	wavelength of surface corrugation	6.0 mm	[103]
k_w	thermal conductivity of plate (copper)	385 W/mK	–

A.1. Single-phase process

For single-phase heat transfer, the Nusselt number is expressed as a function of the Reynolds Re and Prandtl number Pr:

$$Nu = \alpha Re^{b} Pr^{c}, \tag{A.2}$$

with coefficients a, b and c. For Reynolds numbers lower than 1000, the coefficients a, b and c are determined by correlations of Bogaert et al. [105], and for higher Reynolds number they are equal to $0.724(6\ \beta/\pi)^{0.646}$, 0.583 and 0.333 based on the correlation of Chisholm et al. [106].

A.2. Condensation process

For condensation, the Nusselt number is calculated using the correlation of Yan et al. [107]:

$$Nu = 4.118 {Re_{eq}}^{0.4} Pr^{0.667}, \tag{A.3}$$

where:

$$Re_{eq} = \frac{G_{eq} \bullet d_h}{\mu_l}; \tag{A.4}$$

$$G_{eq} = G\left(1 - q + q\left(\frac{\rho_l}{\rho_v}\right)^{0.5}\right); \tag{A.5}$$

$$G = \frac{\dot{m}_{wf}}{A_{chan}}. \tag{A.6}$$

A.4. Absorption process

For absorption, the Nusselt number is calculated based on the correlation of Lee et al. [108]. The same correlation was also used by Mounier [104] for small-scale absorption processes in PHEs:

$$Nu = 3.133 {Re_{sol}}^{0.2519} {Re_v}^{0.2995} \left(\frac{\Delta c}{c_{sol}}\right)^{0.08636} \left(\frac{\Delta T}{T_{sol}}\right)^{0.06851}. \tag{A.7}$$

A.5. Desorption (generator) process

For the generator, the Nusselt number is calculated using the correlation from Táboas et al. [109]:

$$Nu = \frac{5Bo \bullet \alpha_l \bullet d_H}{\lambda_l}, \tag{A.8}$$

where the boiling number Bo is equal to:

$$Bo = \frac{\left(\dot{Q}/A_{chan}\right)}{G \bullet L_{wf}}, \tag{A.9}$$

and α_l is the local heat transfer coefficient of the liquid phase and is calculated using Equation (A.2). The above correlation is only valid based on a superficial vapour velocity criterion that was checked.

Appendix B. . Plate fin-and-tube heat exchanger heat transfer correlations

The geometrical parameters of plate fin-and-tube heat exchangers are based on the work of Lecompte et al. [75] and are shown in Table B.1. Based on these, the number of tubes per row that are required to achieve the required heat transfer of each heat exchanger is identified.

The overall heat transfer coefficient for cross-flow plate fin-and-tube heat exchangers based on the interior surface of the tube is determined by a modified version of Equation (32):

Table B1
Main geometrical parameters used in plate fin-and-tube heat exchanger models.

Parameter	Description	Value	Ref.
H_{fin}	fin height	8.9 mm	[75]
δ_{fin}	fin thickness	0.5 mm	[75]
S_{fin}	fin spacing	2.3 mm	[75]
$D_{tube,out}$	tube outer diameter	15.9 mm	[75]
δ_{tube}	tube thickness	1.5 mm	[75]
S_{tube}	tube spacing	50.0 mm	[75]
n_{rows}	number of rows	4	[110]

$$\frac{1}{U_j}=\frac{1}{\alpha_{wf,j}}+\frac{\delta_{tube}}{k_{tube}}\left(\frac{A_{tube,int}\ln\left(\frac{D_{tube,out}}{D_{tube,int}}\right)}{2\pi l_{tube}}\right)+\frac{A_{tube,int}}{\alpha_{air,j}A_{tube,ext}\eta_o}, \tag{B.1}$$

where $A_{tube,int}$ is the internal tube heat transfer surface area, $A_{tube,ext}$ the total external tube heat transfer area (including fins), $D_{tube,int}$ the tube inner diameter (calculated based on tube outer diameter and thickness), l_{tube} the length of the tubes (which is approximated to be equal to the width of the heat exchanger) and η_o the overall surface efficiency, which is equal to:

$$\eta_o=1-\frac{A'_{fin}}{A'_{tube,ext}}(1-\eta_{fin}), \tag{B.2}$$

where:

$$A'_{tube,ext}=A'_{fin}+A'_{root}; \tag{B.3}$$

$$A'_{fin}=\frac{\pi}{\delta_{fin}+S_{fin}}\left(\frac{D_{fin}{}^2-D_{tube,out}{}^2}{2}+D_{fin}\delta_{fin}\right); \tag{B.4}$$

$$A'_{root}=\pi D_{tube,out}\left(\frac{S_{fin}}{\delta_{fin}+S_{fin}}\right). \tag{B.5}$$

The diameter of the fin D_{fin} is determined using Equation (B.6):

$$D_{fin}=D_{tube,out}+2H_{fin}. \tag{B.6}$$

The fin efficiency η_{fin} is calculated according to the Schmidt approximation [111]:

$$\eta_{fin}=\frac{\tanh(m\varphi D_{tube,out})}{m\varphi D_{tube,out}}, \tag{B.7}$$

where:

$$m=\sqrt{\frac{2\alpha_{air}}{k_{tube}\delta_{fin}}}, \tag{B.8}$$

and:

$$\varphi=\left(\frac{D_{tube,out}+2H_{fin}}{D_{tube,out}}-1\right)\left[1+0.35\ln\frac{D_{tube,out}+2H_{fin}}{D_{tube,out}}\right]. \tag{B.9}$$

For plate fin-and-tube heat exchangers, the hydraulic diameter is determined based on the equation proposed by Mon [110]:

$$d_H=4\left(D_{tube,out}+2H_{fin}\right)\frac{A'_{free}}{A'_{tube,ext}}, \tag{B.10}$$

where $A^{'}_{\text{free}}$ is the minimum free flow area of finned tube per unit length:

$$A^{'}_{\text{free}} = S_{\text{tube}} - D_{\text{fin}} + \left(D_{\text{fin}} - D_{\text{tube,out}}\right)\left(\frac{S_{\text{fin}}}{\delta_{\text{fin}} + S_{\text{fin}}}\right). \tag{B.11}$$

B.1. Single-phase process

For the air-side heat transfer across finned tubes, the Nusselt number is calculated based on the Briggs and Young correlation [112]:

$$Nu = 0.134 Re^{0.68} Pr^{0.333}\left(\frac{H_{\text{fin}}}{S_{\text{fin}}}\right)^{-0.2}\left(\frac{\delta_{\text{fin}}}{S_{\text{fin}}}\right)^{-0.12}. \tag{B.12}$$

B.2. Evaporation process

For evaporation in tubes, Chen's correlation of [113] is used, considering nucleate and convective boiling:

$$\alpha_{\text{wf}} = \alpha_{\text{fc}} + \alpha_{\text{nb}}. \tag{B.13}$$

The forced convection coefficient α_{fc} is estimated using:

$$\alpha_{\text{fc}} = F\alpha_{\text{wf,l}}, \tag{B.14}$$

where $\alpha_{\text{wf,l}}$ is the heat transfer coefficient of the liquid phase, and the forced convection multiplier F is:

$$F = 2.35\left(\frac{1}{X_{\text{tt}}} + 0.213\right)^{0.736}, \tag{B.15}$$

with:

$$X_{\text{tt}} = \left(\frac{1-q}{q}\right)^{0.875}\left(\frac{\rho_{\text{wf,v}}}{\rho_{\text{wf,l}}}\right)^{0.5}\left(\frac{\mu_{\text{wf,l}}}{\mu_{\text{wf,v}}}\right)^{0.125}. \tag{B.16}$$

The Reynolds number of the liquid phase is equal to:

$$Re_{\text{wf,l}} = \frac{\dot{m}_{\text{wf}}(1-q)d_{\text{H}}}{\mu_{\text{wf,l}}}, \tag{B.17}$$

and $\alpha_{\text{wf,l}}$ to:

$$\alpha_{\text{wf,l}} = 0.023\frac{k_{\text{wf,l}}}{D_{\text{tube,int}}} {Re_{\text{wf,l}}}^{0.8} {Pr_{\text{wf,l}}}^{0.333}. \tag{B.18}$$

The nucleate boiling coefficient α_{nb} is estimated using:

$$\alpha_{\text{nb}} = S_{\text{f}}\alpha_{\text{fz}}, \tag{B.19}$$

where:

$$\alpha_{\text{fz}} = \frac{0.00122 {\Delta T_{\text{sat}}}^{0.24} {\Delta P_{\text{sat}}}^{0.75} {c_{\text{p,wf,l}}}^{0.45} {\rho_{\text{wf,l}}}^{0.45} {k_{\text{wf,l}}}^{0.45}}{{\sigma_{\text{wf}}}^{0.5} {L_{\text{wf}}}^{0.24} {\mu_{\text{wf,l}}}^{0.29} {\rho_{\text{wf,g}}}^{0.24}}; \tag{B.20}$$

$$S_{\text{f}} = \frac{1}{1 + 2.53 \bullet 10^{-0.6} {Re_{\text{wf}}}^{1.17}}; \tag{B.21}$$

$$\Delta T_{\text{sat}} = T_{\text{w}} - T_{\text{sat}}; \tag{B.22}$$

$$\Delta P_{\text{sat}} = P_{\text{sat}}\left\{e^{\frac{L_{\text{wf}} M}{R}\left(\frac{1}{T_{\text{sat}}} - \frac{1}{T_{\text{w}}}\right)} - 1\right\}; \tag{B.23}$$

$$Re_{\text{wf}} = F^{1.25} Re_{\text{wf,l}}. \tag{B.24}$$

References

[1] Fankhauser S, Smith SM, Allen M, Axelsson K, Hale T, Hepburn C, et al. The meaning of net zero and how to get it right. Nat Clim Chang 2022;12:15–21.
[2] International Energy Agency. Global status report for buildings and construction. 2019. https://www.worldgbc.org/news-media/2019-global-status-report-buildings-and-construction.
[3] Department for Business, Energy and Industrial Strategy. Net Zero – Technical report. 2019. https://www.theccc.org.uk/publication/net-zero-technical-report.
[4] HM Government. Net Zero Strategy: Build Back Greener, 2021. https://www.gov.uk/government/ publications/net-zero-strategy.
[5] Chowdhury K. Decarbonising the residential space heating sector of the Netherlands in 2050 through three decarbonisation pathways: hydrogen boilers, hybrid heat pumps and electric heat pumps. TU Delft Thesis 2020.
[6] Gross R, Hanna R. Path dependency in provision of domestic heating. Nat Energy 4: 358-64.
[7] Nowak T. Heat pumps – Integrating technologies to decarbonise heating and cooling. European Copper Institute 2018. https://www.ehpa.org/fileadmin/red/03._Media/Publications/ehpa-white-paper-111018.pdf.
[8] Sunny N, Mac Dowell N, Shah N. What is needed to deliver carbon-neutral heat using hydrogen and CCS? Energy Environ Sci 2020;13:4204–24.
[9] European Heat Pump Association. European heat pump market data. 2021. https://www.ehpa.org/market-data.
[10] Greater London Authority. Low carbon heat: heat pumps in. London 2018. https://www.icax.co.uk/pdf/Low_Carbon_Heat-Heat_Pumps_in_London.pdf.
[11] Olympios AV, Pantaleo AM, Sapin P, Markides CN. On the value of combined heat and power (CHP) systems and heat pumps in centralised and distributed heating systems: Lessons from multi-fidelity modelling approaches. Appl Energy 2020;274:115261.
[12] Wilson IAG, Rennie AJR, Ding Y, Eames PC, Hall PJ, Kelly NJ. Historical daily gas and electrical energy flows through Great Britain's transmission networks and the decarbonisation of domestic heat. Energy Policy 2013;61:301–5.
[13] Liu Y, Yang L, Zheng W, Liu T, Zhang X, Liu J. A novel building energy efficiency evaluation index: Establishment of calculation model and application. Energy Convers Manag 2018;166:522–33.
[14] Walker I, Hope A. Householders' readiness for demand-side response: A qualitative study of how domestic tasks might be shifted in time. Energy Build 2020;215:109888.
[15] Dong S, Kremers E, Brucoli M, Rothman R, Brown S. Techno-enviro-economic assessment of household and community energy storage in the UK. Energy Convers Manag 2020;205:112330.
[16] Hutty TD, Patel N, Dong S, Brown S. Can thermal storage assist with the electrification of heat through peak shaving? Energy Rep 2020;6:124–31.
[17] Olympios AV, McTigue JD, Farres-Antunez P, Tafone A, Romagnoli A, Li Y, et al. Progress and prospects of thermo-mechanical energy storage – a critical review. Prog Energy 2021;3:022001.
[18] Element Energy. Hydrogen supply chain: evidence base. 2018. https://www.gov.uk/government/publications/hydrogen-supply-chain-evidence-base.
[19] Energy Networks Association. Britain's hydrogen network plan. 2021. https://www.energynetworks.org/industry-hub/resource-library/britains-hydrogen-network-plan.pdf.
[20] E.ON Group. 20 percent hydrogen in the German gas network for the first time. 2021. https://www.eon.com/en/about-us/media/press-release/2021/20-percent-hydrogen-in-the-german-gas-network-for-the-first-time.html.
[21] The Engineer. Big Four make price promise on domestic hydrogen boilers. 2021. https://www.theengineer.co.uk/big-four-make-price-promise-on-domestic-hydrogen-boilers.
[22] Mac Dowell N, Sunny N, Brandon N, Herzog H, Ku YA, Maas W, et al. The hydrogen economy: A pragmatic path forward. Joule 2021;5(10):2524–9.
[23] Daggash HA, Fajardy M, Mac DN. Chapter 14: Negative emissions technologies. Carbon Capture and Storage. The Royal Society of Chemistry; 2020.
[24] Collodi G, Azzaro G, Ferrari N, Santos S. Techno-economic evaluation of deploying CCS in SMR based merchant H_2 Production with NG as feedstock and fuel. Proc: 13th International Conference on Greenhouse Gas Control Technologies. 2017.
[25] Masoudi Soltani S, Lahiri A, Bahzad H, Clough P, Gorbounov M, Yan Y. Sorption-enhanced steam methane reforming for combined CO_2 capture and hydrogen production: A state-of-the-art review. Carbon Capture Sci Technol 2021;1:100003.
[26] Huang WJ, Yu CT, Sheu WJ, Chen YC. The effect of non-uniform temperature on the sorption-enhanced steam methane reforming in a tubular fixed-bed reactor. Int J Hydrogen Energy 2021;46(31):16522–33.
[27] Sheu WJ, Chu CS, Chen YC. The operation types and operation window for high-purity hydrogen production for the sorption enhanced steam methane reforming in a fixed-bed reactor. Int J Hydrogen Energy 2021.
[28] Secretary of State for Business, Energy and Industrial Strategy. UK hydrogen strategy. 2021. https://www.gov.uk/government/publications/uk-hydrogen-strategy.
[29] Sadler D, Anderson HS, Sperrink M, Cargill A. H21 North of England. 2018. https://h21.green/projects/h21-north-of-england.
[30] Scoccia R, Toppi T, Aprile M, Motta M. Absorption and compression heat pump systems for space heating and DHW in European buildings: Energy, environmental and economic analysis. J Build Eng 2018;16:94–105.
[31] Toppi T, Aprile M, Motta M, Bongs C. Seasonal performance calculation and transient simulation of a newly developed 18 kW air-source water-ammonia gas heat pump for residential applications. In Proc: 11th International Energy Agency (IEA) Heat Pump Conference, Montreal, Canada; 2014.
[32] Lu D, Bai Y, Dong X, Zhao Y, Guo H, Gong M. Gas-fired absorption heat pump applied for high-temperature water heating: Parametric study and economic analysis. Int J Refrig 2020;119:152–64.
[33] Wu W, Ran S, Shi W, Wang B, Li X. NH_3 -H_2O water source absorption heat pump (WSAHP) for low temperature heating: Experimental investigation on the off-design performance. Energy 2016;115:697–710.
[34] Ayou DS, Eveloy V. Energy, exergy and exergoeconomic analysis of an ultra low-grade heat-driven ammonia-water combined absorption power-cooling cycle for district space cooling, sub-zero refrigeration, power and LNG regasification. Energy Convers Manag 2020;213:112790.
[35] Najjaran A, Freeman J, Ramos A, Markides CN. Experimental investigation of an ammonia-water-hydrogen diffusion absorption refrigerator. Appl Energy 2019;256:113899.
[36] Fernández-Seara J, Sieres J. The importance of the ammonia purification process in ammonia-water absorption systems. Energy Convers Manag 2006;47:1975–87.
[37] Aprile M, Scoccia R, Toppi T, Guerra M, Motta M. Modelling and experimental analysis of a GAX NH_3-H_2O gas-driven absorption heat pump. Int J Refrig 2016;66:145–55.
[38] The Carbon Trust, Rawlings Support Services. Evidence gathering - low carbon heating technologies - domestic high temperature heat pumps. 2016. https://www.gov.uk/government/publications/evidence-gathering-high-temperature-heat-pumps-hybrid-heat-pumps-and-gas-driven-heat-pumps.
[39] Song J, Olympios AV, Mersch M, Sapin P, Markides CN. Integrated organic Rankine cycle (ORC) and heat pump (HP) systems for domestic heating. In Proc: 34th International Conference on Efficiency, Costs, Optimization, Simulation and Environmental Impact of Energy Systems (ECOS 2021), Taormina, Italy; 2021.
[40] Baldi S, Le Quang T, Holub O, Endel P. Real-time monitoring energy efficiency and performance degradation of condensing boilers. Energy Convers Manag 2017;136:329–39.
[41] Garrabrant M, Stout R, Glanville P, Fitzgerald J, Keinath C. Development and validation of a gas-fired residential heat pump water heater. 2013. https://www.osti.gov/servlets/purl/1060285.
[42] Critoph R, Metcalf S UK Summary Report on IEA Heat Pump Technology Collaboration Programme (TCP) Annex 43: Thermally Driven Heat Pumps. Department for Business, Energy and Industrial Strategy; 2019. https://www.gov.uk/government/publications/fuel-driven-heat-pumps.
[43] Pudjianto D, Aunedi M, Djapic P, Strbac G. Whole-systems assessment of the value of energy storage in low-carbon electricity systems. IEEE Trans Smart Grid 2014;5(2):1098–109.
[44] Strbac G, Pudjianto D, Sansom R, Djapic P, Ameli H, Shah N, Hawkes A. Analysis of Alternative UK Heat Decarbonisation Pathways. 2018. https://www.theccc.org.uk/wp-content/uploads/2018/06/Imperial-College-2018-Analysis-of-Alternative-UK-Heat-Decarbonisation-Pathways.pdf.
[45] Olympios AV, Hoseinpoori P, Mersch M, Pantaleo AM, Simpson MC, Sapin P, Mac Dowell N, Markides CN. Optimal design of low-temperature heat-pumping technologies and implications to the whole- energy system. In Proc: 33rd International Conference on Efficiency, Costs, Optimization, Simulation and Environmental Impact of Energy Systems (ECOS 2020), Osaka, Japan; 2020.
[46] Olympios AV, Pantaleo AM, Sapin P, van Dam KH, Markides CN. Centralised vs distributed energy systems options: district heating for the Isle of Dogs in London. In Proc: 11th International Conference on Applied Energy (ICAE 2019), Västerås, Sweden, 2019.
[47] Roy R, Bhowal AJ, Mandal BK. Exergy and cost optimization of a two-stage refrigeration system using refrigerant R32 and R410A. J Therm Sci Eng Appl 2020;12(3):031024.
[48] Nhut LM, Danh TQ. An experimental investigation on the coefficient of performance of the small hot water heat pump using refrigeration R410A and R32. Sci Technol Dev J - Eng Technol 2020;3(2):425–31.
[49] Danfoss, Refrigerant Slider, 2021. https://reftools.danfoss.com/spa/tools#.
[50] Olympios AV, Mersch M, Sapin P, Pantaleo MA, Markides CN. Library of price and performance data of domestic and commercial technologies for low-carbon energy systems 2021. https://doi.org/10.5281/zenodo.5758943.
[51] Hepbasli A, Kalinci Y. A review of heat pump water heating systems. Renew Sustain Energy Rev 2009;13(6–7):1211–29.
[52] Ezzat MF, Dincer I. Energy and exergy analyses of a new geothermal-solar energy-based system. Sol Energy 2016;134:95–106.
[53] Kuzgunkaya EH, Hepbasli A. Exergetic performance assessment of a ground-source heat pump drying system. Int J Energy Res 2007;31(8):760–77.
[54] Dodds PE, Staffell I, Hawkes AD, Li F, Grünewald P, McDowall W, et al. Hydrogen and fuel cell technologies for heating: A review. Int J Hydrogen Energy 2015;40:2065–83.
[55] Terhan M, Comakli K. Energy and exergy analyses of natural gas-fired boilers in a district heating system. Appl Therm Eng 2017;121:380–7.
[56] Ciniviz M, Köse H. Hydrogen use in internal combustion engine: a review. Int J Automot Eng Technol 2012;1(1):1–15.
[57] Giacomini. H2ydroGEM, the hydrogen boiler by Giacomini, 2021. https://www.giacomini.com/en/hydrogen-systems/h2ydrogem-hydrogen-boiler-giacomini.
[58] The MathWorks Inc. MATLAB R2021a. Natick, Massachusetts; 2021.
[59] Lemmon E, Huber ML, McLinden MO. NIST Standard reference database 23: Reference fluid thermodynamic and transport properties-REFPROP. Version 2018;10.
[60] M Conde Engineering. Thermophysical properties of NH_3 + H_2O mixtures for the industrial design of absorpion refrigeration equipment: Formulation for industrial use. Zurich, Switzerland, 2006.

[61] Esfahani JI, Tae Y, Yoo C. A high efficient combined multi-effect evaporation-absorption heat pump and vapor-compression refrigeration part 1: Energy and economic modeling and analysis. Energy 2014;75:312–26.
[62] Misra RD, Sahoo PK, Sahoo S, Gupta A. Thermoeconomic otimization of a single effect 64/LiBr vapour absorption refrigeration system. Int J Refrig 2003;26(2):158–69.
[63] Wu C, Wang S, Feng X, Li J. Energy, exergy and exergoeconomic analyses of a combined supercritical CO_2 recompression Brayton/absorption refrigeration cycle. Energy Convers Manag 2017;148:360–77.
[64] Gebreslassie BH, Guillén-gosálbez G, Jiménez L, Boer D. Design of environmentally conscious absorption cooling systems via multi-objective optimization and life cycle assessment. Appl Energy 2009;86(9):1712–22.
[65] Garousi Farshi L, Mahmoudi SMS, Rosen MA. Exergoeconomic comparison of double effect and combined ejector-double effect absorption refrigeration systems. Appl Energy 2013;103:700–11.
[66] Bakhtiari B, Fradette L, Legros R, Paris J. A model for analysis and design of H_2O-LiBr absorption heat pumps. Energy Convers Manag 2011;52(2):1439–48.
[67] Jain V, Sachdeva G. Energy, exergy, economic (3E) analyses and multi-objective optimization of vapor absorption heat transformer using NSGA-II technique. Energy Convers Manag 2017;148:1096–113.
[68] Gebreslassie BH, Groll EA, Garimella SV. Multi-objective optimization of sustainable single-effect water / lithium bromide absorption cycle. Renew Energy 2012;46:100–10.
[69] Jernqvist Å, Abrahamsson K, Aly G. On the efficiencies of absorption heat pumps. Heat Recover Syst CHP 1992;12(6):469–80.
[70] Wu Z, You S, Zhang H, Wang Y, Wei S, Jiang Y, et al. Performance analysis and optimization for a novel air-source gas-fired absorption heat pump. Energy Convers Manag 2020;223:113423.
[71] Bolaji BO, Huan Z. Ozone depletion and global warming: Case for the use of natural refrigerant – a review. Renew Sustain Energy Rev 2013;18:49–54.
[72] Turton R, Bailie RC, Whiting WB, Shaeiwitz JA, Bhattacharyya D. Analysis, synthesis, and design of chemical processes. Fourth ed. London: Pearson Education International; 2012.
[73] Wang Y, Song J, Chatzopoulou MA, Sunny N, Simpson MC, Wang J, et al. A holistic thermoeconomic assessment of small-scale, distributed solar organic Rankine cycle (ORC) systems: Comprehensive comparison of configurations, component and working fluid selection. Energy Convers Manag 2021;248:114618.
[74] Guo K. Optimisation of plate/plate-fin heat exchanger design. The University of Manchester PhD Thesis. 2015.
[75] Lecompte S, Huisseune H, van den Broek M, De Schampheleire S, De Paepe M. Part load based thermo-economic optimization of the Organic Rankine Cycle (ORC) applied to a combined heat and power (CHP) system. Appl Energy 2013;111:871–81.
[76] Stewart SW. Enhanced finned-tube condenser design and optimization. Georgia Institute of Technology PhD Thesis 2003.
[77] iACS. Carel refrigeration valves. 2021. https://www.i-acs.co.uk/store/products/expansion-valves-drivers/refrigeration-valves.html.
[78] Department of Energy and Climate Change. Potential cost reductions for air source heat pumps. 2016. https://assets.publishing.service.gov.uk/government/uploads/system/uploads/attachment_data/file/498962/150113_Delta-ee_Final_ASHP_report_DECC.pdf.
[79] Department of Energy and Climate Change. Assessment of the costs, performance, and characteristics of UK heat networks. 2015. https://assets.publishing.service.gov.uk/government/uploads/system/uploads/attachment_data/file/424254/heat_networks.pdf.
[80] Department for Business, Energy and Industical Strategy. Heat networks consumer survey: Results Report. 2017. https://assets.publishing.service.gov.uk/government/uploads/system/uploads/attachment_data/file/665447/HNCS_Results_Report_-_FINAL.pdf.
[81] Kiptoo MK, Lotfy ME, Adewuyi OB, Conteh A, Howlader AM, Senjyu T. Integrated approach for optimal techno-economic planning for high renewable energy-based isolated microgrid considering cost of energy storage and demand response strategies. Energy Convers Manag 2020;215:112917.
[82] Wang K, Herrando M, Pantaleo AM, Markides CN. Technoeconomic assessments of hybrid photovoltaic-thermal vs. conventional solar-energy systems: Case studies in heat and power provision to sports centres. Appl Energy 2019;254:113657.
[83] Department of Business, Energy and Industrial Strategy. Cost of installing heating measures in domestic properties, 2020. https://www.gov.uk/government/publications/cost-of-installing-heating-measures-in-domestic-properties.
[84] Local Heros. How much does a boiler service cost? 2021. https://www.localheroes.com/advice/how-much-boiler-service.
[85] Triami Media BV. Inflation by country/region. 2022. https://www.inflation.eu/en/inflation-rates/cpi-inflation-2021.aspx.
[86] Sansom R. Decarbonising low grade heat for low carbon future. Imperial College London PhD Thesis 2014.
[87] Zhang X, Strbac G, Shah N, Teng F, Pudjianto D. Whole-System assessment of the benefits of integrated electricity and heat system. IEEE Trans Smart Grid 2018;10(1):1132–45.
[88] European Commission. Photovoltaic Geographical information system (PVGIS). 2020. https://ec.europa.eu/jrc/en/pvgis.
[89] Gleeson C, Biddulph P, Lowe R, Love J, Summerfield A, Oikonomou E, Wingfield J, Martin C. Analysis of heat pump data from the renewable heat premium payment scheme to the Department of Business, Energy and Industrial Strategy: Compliance with MCS Installation Standards. UCL Energy Institute. 2017. https://www.gov.uk/government/publications/detailed-analysis-of-data-from-heat-pumps-installed-via-the-renewable-heat-premium-payment-scheme-rhpp.
[90] Eco Heating System Samsung. Powerful and eco-friendly air to water solutions for heating 2018. https://www.heatpumpsscotland.com/wp-content/uploads/2018/06/Energy-Labelling.pdf.
[91] Xpress-Optimizer. Fico Xpress Optimization, 2021. https://www.fico.com/en/products/fico-xpress-optimization.
[92] Department of Business, Energy and Industrial Strategy. Hydrogen production costs. 2021. https://www.gov.uk/government/publications/hydrogen-production-costs-2021.
[93] Department of Business, Energy and Industrial Strategy. Electricity generation costs. 2020. https://www.gov.uk/government/publications/beis-electricity-generation-costs-2020.
[94] Climate Change Committee. The Sixth Carbon Budget: The UK's path to Net Zero. 2020. https://www.theccc.org.uk/publication/sixth-carbon-budget.
[95] British Standards Institution. BS EN 14511-4: 2018: Air conditioners, liquid chilling packages and heat pumps for space heating and cooling and process chillers, with electrically driven compressors- Test conditions. 2018.
[96] Baldino C, Searle S, Zhou Y, Christensen A. Hydrogen for heating? Decarbonization options for households in the United Kingdom in 2050. International Council of Clean Transportation 2020.
[97] Gérard F, van Nuffel L, Smit T, Yearwood J, Černý O, Michalski J, Altmann M. Opportunities for hydrogen energy technologies considering the National Energy & Climate Plans. 2020. https://www.fch.europa.eu/publications/opportunities-hydrogen-energy-technologies-considering-national-energy-climate-plans.
[98] Jovan DJ, Dolanc G. Can green hydrogen production be economically viable under current market conditions. Energies 2020;13(24):6599.
[99] European Energy Research Alliance. Joint research programme on fuel cells and hydrogen technologies: Implementation plan 2018 – 2030. 2019. https://www.eera-set.eu/component/attachments/?task=download&id=253.
[100] Hydrogen Europe. Strategic research and innovation agenda. 2020. https://hydrogeneurope.eu/reports.
[101] Statista. Electricity prices for households in the United Kingdom. 2021. https://www.statista.com/statistics/418126/electricity-prices-for-households-in-the-uk.
[102] Alfa Laval. CB16 / CBH16 Brazed plate heat exchanger, 2021. https://www.alfalaval.com/globalassets/documents/microsites/heating-and-cooling-hub/pd-leaflets/cb16_product-leaflet.pdf.
[103] Asadi M, Khoshkhoo RH. Effects of wavelength on the thermal performance of a plate heat exchanger. Therm Eng 2013;60:16603–8.
[104] Mounier V, Mendoza LC, Schiffmann J. Thermo-economic optimization of an ORC driven heat pump based on small scale turbomachinery and comparison with absorption heat pumps. Int J Refrig 2017;81:96–110.
[105] Bogaert R, Böles A. Global performance of a prototype brazed plate heat exchanger in a large reynolds number range. Exp Heat Transf 1995;8(4):293–311.
[106] Chisholm D, Wanniarachchi AS. Layout of plate heat exchangers. In Proc: ASME/JSME Thermal Engineering Joint Conference, Reno, Nevada; 1991.
[107] Yan YY, Lio HC, Lin TF. Condensation heat transfer and pressure drop of refrigerant R-134a in a plate heat exchanger. Int J Heat Mass Transf 1999;42(6):993–1006.
[108] Lee KB, Chun BH, Lee JC, Lee CH, Kim SH. Experimental analysis of bubble mode in a plate-type absorber. Chem Eng Sci 2002;57(11):1923–9.
[109] Táboas F, Vallès M, Bourouis M, Coronas A. Assessment of boiling heat transfer and pressure drop correlations of ammonia/water mixture in a plate heat exchanger. Int J Refrig 2012;35(3):633–44.
[110] Mon MS. Numerical investigation of air-side heat transfer and pressure drop in circular finned-tube heat exchangers. TU Bergakademie Freiberg PhD Thesis 2003.
[111] Schmidt TE. Heat transfer calculations for extended surfaces. Refrig Eng 1949;57:351–7.
[112] Briggs DE, Young EH. Convection heat transfer and pressure drop of air flowing across triangular pitch banks of finned tubes. Chem Eng Prog Symp Ser 1963;59(41):1–10.
[113] Chen JC. Correlation for boiling heat transfer to saturated fluids in convective flow. Ind Eng Chem Process Des Dev 1966;5(3):322–9.